Spatial Price Integration in Commodity Markets with Capacitated Transportation Networks

John R. Birge
Booth School of Business, University of Chicago, Chicago, Illinois, 60637, john.birge@chicagobooth.edu

Timothy C. Y. Chan
Department of Mechanical and Industrial Engineering, University of Toronto, Toronto, Ontario M5S 3G8, Canada, tcychan@mie.utoronto.ca

J. Michael Pavlin
Lazaridis School of Business and Economics, Wilfrid Laurier University, Waterloo, Ontario N2L 3C5, Canada, mpavlin@wlu.ca

Ian Yihang Zhu
Department of Mechanical and Industrial Engineering, University of Toronto, Toronto, Ontario M5S 3G8, Canada, i.zhu@mail.utoronto.ca

Spatial price integration is extensively studied in commodity markets as a means of examining the degree of integration between regions of a geographically diverse market. Many commodity markets that are commonly studied are supported by a well-defined transportation network, such as the network of pipelines in oil and gas markets. In this paper, we analyze the relationship between spatial price integration, i.e., the distribution of prices across geographically distinct locations in the market, and the features of the underlying transportation network. We characterize this relationship and show that price integration is strongly influenced by the characteristics of the transportation network, especially when there are capacity constraints on links in the network. Our results are summarized using a price decomposition which explicitly isolates the influences of market forces (supply and demand), transportation costs and capacity constraints among a set of equilibrium prices. We use these theoretical insights to develop a unique discrete optimization methodology to capture spatiotemporal price variations indicative of underlying network bottlenecks. We apply the methodology to gasoline prices in the southeastern U.S., where the methodology effectively characterizes the effects of a series of well-documented network disruptions on market prices, providing important implications for operations and supply chain management.

Key words: commodity and energy operations; price integration; spatial price equilibrium; supply chain management; network disruptions; congestion; time series analysis; mixed integer programming

1. Introduction

Spatial price integration, defined as the co-movement of prices in a market with geographically separated market participants, is studied extensively in commodity markets. Prices from spatially separated locations that move together are taken as evidence of strong market integration, suggest-

ing that the underlying market is competitive and sufficiently well connected for price differences to be quickly arbitraged away. On the other hand, prices that are not strongly integrated may suggest the existence of frictions such as market power or transportation bottlenecks (Martínez-de Albéniz and Vendrell Simón 2017). Studying and characterizing such frictions have important policy implications for market participants, especially consumers. Given the relative ease of acquiring pricing data (i.e., data of commodity prices) over large geographies, measures of price integration are attractive proxies for market efficiency in large scale studies.

A range of time series econometric methods are typically employed to study market integration in commodity markets; see Dukhanina and Massol (2018) for a review of methods. However, many of these price-based empirical methods are not specific for markets with well-defined logistical networks but rather for general financial and economic time series data. As a result, a number of studies suggest that caution is needed when applying these price-based methods to study market efficiency in networked markets, i.e., when market participants are connected by well-defined but costly transportation modes. In these markets, it is possible that the assumptions underlying these time series methods may not be consistent with the spatial equilibrium conditions governing the structural model of the market (McNew and Fackler 1997, Fackler and Tastan 2008, Dukhanina and Massol 2018). The most notable example illustrating this inconsistency is the notion of a *neutral band* existing between prices at two locations with costly bidirectional transportation (e.g., Goodwin and Piggott 2001). Large price variations can occur within a neutral band defined by the transportation costs without an error-correction (i.e., arbitrage) mechanism, even when the market is efficient. In this pairwise setting, it has been shown that the concept of co-integration is neither necessary nor sufficient for the identification of unexploited arbitrage opportunities or bottlenecks (McNew and Fackler 1997), highlighting the importance of considering the structural equilibrium conditions when studying price integration in a market.

In this paper, we aim to provide a deeper understanding of spatial price integration in markets with well-defined transportation networks. Our work is particularly relevant for energy markets, where locations typically trade through stable transportation networks such as the network of fossil-fuel pipelines or railroads for tank cars. In this setting, we establish a fundamental connection between structural characteristics of a market and spatial price integration, which we use to derive principled methods for market analysis.

We model the market as a network with nodes representing market participants and directed links representing transportation. We study price formation using a spatial price equilibrium model (SPE), which we use to characterize the relationship between prices and market structure. The results extend the neutral band concept, previously examined only for pairs of nodes with direct

connections (i.e., "pairwise" neutral band) to uncapacitated networks where nodes may be connected indirectly through a series of links (i.e., "network" neutral band). We then focus on price integration in the presence of capacitated links. In many countries where commodity markets have undergone significant deregulatory changes, such as those found in the oil and gas markets, bottlenecks generated by limited capacity in the transportation network are arguably the last remaining prevalent source of major market inefficiencies (Oliver et al. 2014). We study how price shocks generated from bottlenecks are distributed over the market. We then leverage the results of the SPE model to generate a principled and scalable empirical methodology to identify these shocks in the market. Our methodology uses spatial pricing data to identify time periods and locations with temporarily inflated prices indicative of capacity constraints in the transportation network. Finally, we demonstrate through a numerical case study using pricing data alone that our methodology accurately identifies spatiotemporal variations consistent with well-documented disruptions in the Southeastern U.S. gasoline market. For the remainder of the paper, we use the term *market structure* to refer to the transportation network, which is defined by the network structure (nodes and links), transportation costs on the links, and link capacities.

Our specific contributions and their organization within the paper are as follows:

1. We provide a novel characterization of the relationship between market structure and price integration over general transportation networks. Our results are derived with arbitrary demand and supply functions allowing us to isolate the effect that different components of the market structure have on bounding price differences within the market.
   (a) Uncapacitated and costless transportation (Section 4.1): We show that a structural property of the network, defined as *structural integration*, is a necessary and sufficient condition for the *law of one price* to hold over the nodes.
   (b) Uncapacitated but costly transportation (Section 4.2): We prove existence of a *network neutral band*, which bounds the distribution of prices over the market, and is entirely characterized by the parameters of the network and is independent of the market participants. This result extends the *pairwise neutral band* concept to pairs of non-adjacent nodes in the network.
   (c) Capacitated and costly transportation (Section 4.3): We characterize how nodal prices incorporate *congestion surcharges* throughout the network. In particular, we relate these surcharges to the shadow price of capacity constraints in the underlying efficient allocation problem.
2. Using the previous insights, we identify a novel decomposition of the nodal prices that we use to develop a *surcharge estimation model* (SEM), a unique discrete optimization approach for time series analysis. The SEM is a tractable and interpretable methodology for capturing

market characteristics and spatiotemporal variations in spatial time series pricing data that are indicative of bottleneck constraints in the underlying market (Section 5).

3. We present a comprehensive case study of the Southeastern U.S. gasoline market, where we show that our methodology can accurately identify spatiotemporal variations in prices that are consistent with well-documented disruptions (Section 6). The results provide quantitative estimates for the cost of the disruption to consumers while highlighting how alternative modes of transportation and increases in capacity can mitigate large price shocks in the presence of network bottlenecks.

The main results in the paper are presented under the assumption that the underlying network structure is unchanged over a given time horizon. Thus, our analysis lends itself particularly well to energy markets where the market structure (e.g., the network of pipelines) is generally fixed in the short-term. All proofs are placed in the Appendix.

2. Literature Review

The analytical results and empirical methods we develop in this paper are built on spatial price equilibrium models. We begin this section by discussing both general purpose SPE models and their applications to energy markets. We then contrast our approach with current econometric methods and their applications in energy markets.

2.1. Equilibrium models

Many equilibrium models exist for markets with spatially separated participants, each requiring different assumptions about underlying market conditions; a review of some fundamental spatial models is provided by Harker (1986). We focus on spatial price equilibrium (SPE) models which were introduced in the seminal papers of Samuelson (1952) and Takayama and Judge (1964). SPE models assume a competitive market built over a logistical network where participants are sited at nodes and transportation routes are defined by links between nodes. The equilibrium conditions (i.e., the SPE model) are characterized by the Karush-Kuhn-Tucker (KKT) optimality conditions of the welfare maximizing allocation (optimization) problem.

SPE models have been used extensively for modeling and analysis in energy markets, such as coal (Harker and Friesz 1985), natural gas (Gabriel et al. 2000), crude oil (Bennett and Yuan 2017), and petroleum (Mudrageda and Murphy 2008). Especially relevant are works which focus on capacity constraints in these models. For example, Secomandi (2010) studies the optimal pricing of pipeline capacity in relation to the market participants, whereas Lochner (2011) and Dieckhöner et al. (2013) develop models for counterfactual analysis of the effects of bottleneck constraints on consumer prices over varying forecasts of demand and supply. In contrast, we aim to provide a general

characterization of equilibrium prices specifically in relation to the transportation network (i.e., over arbitrary supply and demand functions), paying special attention to how this characterization can be used for empirical time series analysis.

An important concept arising from these equilibrium models is that of a neutral band, defining a range of price differences where arbitrage is not possible as a result of transaction costs to trade. In commodity markets this transaction cost is primarily the result of transportation costs (e.g. Ejrnaes and Persson 2000, Goletti et al. 1995). To the best of our knowledge however, the study of the neutral band has been limited to pairwise settings where a pair of locations can trade directly. However, when a market is connected by a more general transportation network, as is common in energy markets such as fossil fuel markets, direct links may not exist between each pair of locations. We introduce the concept of *network* neutral bands in this paper to describe price relationships between nodes over general network topologies.

2.2. Econometric methods

While a wide variety of econometric time series methods have been applied to the study of price integration in commodity markets, the most common assessment methods continue to be co-integration tests. Co-integration tests, reviewed in Hendry and Juselius (2000) and Hendry and Juselius (2001), test for the existence of a long-run linear relationship between a set of prices by examining whether deviations from this long-run relationship are stationary. Such tests have been applied widely to analyze market integration and frictions in U.S. gasoline and natural gas markets (e.g. De Vany and Walls 1993, Paul et al. 2001, Brown and Yücel 2008, Holmes et al. 2013). Typically these methods are applied pairwise to assess integration between two regions in the market footprint.

Several shortcomings of these methods have been pointed out in the literature. The most important concern is that requirements for co-integrated prices may not be consistent with economic equilibrium conditions even when the market has active arbitrageurs. As discussed previously, large deviations can occur without an error-correction mechanism as long as the deviations have not exceeded a transaction cost such as the cost of transportation (Lo and Zivot 2001). In this setting, the application of these tests can result in unreliable conclusions on the efficiency of the market (McNew and Fackler 1997). In light of these concerns, threshold models have been proposed which allow for the existence of a band within which deviations from long-run equilibrium may occur without error-correction (e.g. Balke and Fomby 1997). Co-integration is measured only when deviations exceed the threshold. These models have been applied in several commodity markets (e.g. Goodwin and Piggott 2001, Park et al. 2007), limited again to pairwise comparisons. Beyond pairwise analysis, these threshold models offer no definitive or interpretable connection with the logistical network underlying the market.

The methods presented above use only pricing data which is generally broadly available. Market efficiency is also studied using more granular models with additional market data. One popular method is the regime switching model, which is often applied over different commodity markets to estimate the frequency of being in regimes with unexploited arbitrage opportunities by using precise estimates of transportation data; examples include Barrett and Li (2002), Negassa and Myers (2007), and Massol and Banal-Estañol (2016). While these models may be richer, building accurate models and collecting precise data is challenging. In practice, proxies of variables (such as flow values, capacity constraints, and transportation costs) are used, because the actual data is unavailable or confidential. These challenges limit the models to more isolated environments, such as the pair of regions joined by a single pipeline segment (e.g. Oliver et al. 2014, Massol and Banal-Estañol 2016). We instead study market integration using only spatial time series pricing data. From an econometric perspective, we relate the congestion within the logistical structure to particular spatiotemporal patterns in market prices and propose methods for isolating these patterns from readily available pricing data.

3. Market Model and Equilibrium Conditions

In this section, we present a model of a competitive market with transportation capacity constraints and review how the optimality conditions of the associated market allocation problem determine market outcomes and equilibrium prices.

We begin by developing a model of a competitive market for a single commodity with spatially separated market participants. Let the market be represented as a network with a set of nodes $\mathcal{N}$ and a set of directed links $\mathcal{E}$. Consumers are located at nodes $\mathcal{S}$ and producers are located at nodes $\mathcal{K}$, which together form a partition of $\mathcal{N}$. Each consumer node may represent many independent, individual consumers in close spatial proximity (e.g., individual car owners purchasing gas within the same city); the same is true for producer nodes. Each consumer node $s \in \mathcal{S}$ obtains welfare $W_s(b_s)$ when consuming b_s units of the commodity, representing the aggregate welfare of individual consumers comprising node s. Similarly, each producer node $k \in \mathcal{K}$ bears a production cost $W_k(b_k)$ for b_k units of the commodity produced. We assume that the welfare function $W_s(\cdot)$ is strictly concave, increasing, and differentiable, while the cost function $W_k(\cdot)$ is convex, increasing and differentiable. The concavity and convexity assumptions are consistent with standard diminishing marginal utility and diminishing return assumptions from the economics literature. Note that the derivative of the welfare and cost functions, i.e., $W_s'(b_s)$ and $W_k'(b_k)$, are the inverse demand and inverse supply functions at a node s and k, respectively; an increase in demand (supply) results in an increase (decrease) in the welfare (cost) functions for a fixed value b_s (b_k). Finally, rather than explicitly modeling storage facilities, we assume they are co-located with demand and supply

nodes and on a short-term basis behave similarly to other market participants in that they may influence the aggregate production cost or welfare function at their node. For simplicity, we will frequently refer to consumer nodes and producer nodes simply as consumers and producers.

Nodes are connected by a set of transportation links $\mathcal{E}$. Links will be denoted by either e or (i,j), depending on whether explicit reference to the incident nodes of the link is required. The variable f_{ij} represents the flow of the commodity from node i to j on link $(i,j) \in \mathcal{E}$. We use $I_{(i)} = \{n \in N \mid (n,i) \in \mathcal{E}\}$ to denote the set of incoming nodes to i. Similarly, $O_{(i)} = \{n \in N \mid (i,n) \in \mathcal{E}\}$ is the set of outgoing nodes from i. The flow on each link is non-negative, bounded above by the capacity of the link, u_{ij}, and has a non-negative, per-unit transportation cost of c_{ij}. We use $\mathcal{P}_{(i,j)}$ to denote the set of paths from node i to j, where each element of $\mathcal{P}_{(i,j)}$ represents a sequence of links, and p^q_{ij} to denote the cost of a path $q \in \mathcal{P}_{(i,j)}$, which is the sum of the costs on each link in q. For each pair of nodes i and j, let $\mathcal{P}^*_{(i,j)}$ describe the set of minimum-cost paths between i and j, and p^*_{ij} denote the cost of a minimum-cost path. Finally, for a specific consumer $s \in \mathcal{S}$, we let the set $\mathcal{K}_{(s)} \subseteq \mathcal{K}$ denote the set of producer nodes with a directed path to s.

Using the above notation, the equilibrium of the associated competitive market can be modeled using the following welfare-maximizing market allocation problem:

$$\begin{aligned}
\underset{\mathbf{f},\mathbf{b}}{\text{maximize}} \quad & \sum_{s\in\mathcal{S}} W_s(b_s) - \sum_{(i,j)\in\mathcal{E}} c_{ij} f_{ij} - \sum_{k\in\mathcal{K}} W_k(b_k) \\
\text{subject to} \quad & -b_s + \sum_{i\in I(s)} f_{si} - \sum_{j\in O(s)} f_{sj} = 0, \quad \forall s \in \mathcal{S}, \\
& b_k + \sum_{i\in I(k)} f_{ik} - \sum_{j\in O(k)} f_{kj} = 0, \quad \forall k \in \mathcal{K}, \\
& 0 \le f_{ij} \le u_{ij}, \quad \forall (i,j) \in \mathcal{E}, \\
& b_s \ge 0, \quad \forall s \in \mathcal{S}, \\
& b_k \ge 0, \quad \forall k \in \mathcal{K}.
\end{aligned} \tag{1}$$

The equilibrium market allocation in a competitive market maximizes the total social welfare, which, as presented in model (1), is the total consumer welfare minus transportation and production costs (Harker 1986). The first two sets of constraints are the standard flow-balance equations, where consumers and producers withdraw and inject the commodity into the market, respectively. The third constraint represents capacity constraints on flow. Given that $W_s(\cdot)$ and $W_k(\cdot)$ are strictly concave and convex functions, respectively, formulation (1) is a bounded, convex optimization problem. Equilibrium prices can be deduced from the optimality conditions of (1), which are shown below:

$$\lambda_s = W_s'(b_s) + \alpha_s, \quad \forall s \in \mathcal{S}, \tag{2a}$$

$$\lambda_k = W_k'(b_k) - \alpha_k, \quad \forall k \in \mathcal{K}, \tag{2b}$$

$$\lambda_j - \lambda_i = c_{ij} - w_{ij} + \nu_{ij}, \quad \forall (i,j) \in \mathcal{E}, \tag{2c}$$

$$0 \le w_{ij} \perp f_{ij} \ge 0, \quad \forall (i,j) \in \mathcal{E}, \tag{2d}$$

$$0 \le \nu_{ij} \perp (u_{ij} - f_{ij}) \ge 0, \quad \forall (i,j) \in \mathcal{E}, \tag{2e}$$

$$0 \le \alpha_s \perp b_s \ge 0, \quad \forall s \in S, \tag{2f}$$

$$0 \le \alpha_k \perp b_k \ge 0, \quad \forall k \in \mathcal{K}. \tag{2g}$$

We use $\perp$ to define a complementarity constraint. The non-negative variables λ_s and λ_k are the dual variables corresponding to the two sets of flow balance constraints and represent the marginal cost of obtaining a unit of the commodity at the respective nodes; these variables correspond to *equilibrium prices* at the nodes. The variables α_s and α_k are dual variables of the lower bound constraints of b_s and b_k, respectively. The variables w_{ij} and ν_{ij} are the dual variables corresponding to the lower and upper bound constraints on the flow variables, respectively. Following Cremer et al. (2003), we refer to ν_{ij} as the *shadow price* of the capacity constraint on link (i,j). Equation (2c) establishes a connection between the prices at two nodes connected by a single link. Summing this equation over a path q from node n_1 to n_2 that traverses links in a set $\mathcal{E}_q$ results in

$$\begin{aligned} \lambda_{n_2} - \lambda_{n_1} &= \sum_{(i,j)\in\mathcal{E}_q} c_{ij} - \sum_{(i,j)\in\mathcal{E}_q} w_{ij} + \sum_{(i,j)\in\mathcal{E}_q} \nu_{ij} \\ &= p^q_{n_1 n_2} - \sum_{(i,j)\in\mathcal{E}_q} w_{ij} + \nu^q_{n_1 n_2}, \end{aligned} \tag{3}$$

where $\nu^q_{n_1 n_2} = \sum_{(i,j)\in\mathcal{E}_q} \nu_{ij}$ denotes the sum of shadow prices along path q. Conditions (2d)-(2g) represent the complementary conditions. For example, recall that the variables w_{ij} are non-negative and represent the shadow price of the non-negativity flow constraint. When flow on link (i,j) is positive in an optimal market allocation, the value of w_{ij} must be zero by complementary slackness. Thus, equation (3) can be represented as

$$\lambda_{n_2} - \lambda_{n_1} \le p^q_{n_1 n_2} + \nu^q_{n_1 n_2}, \quad \forall q \in \mathcal{P}(n_1, n_2), \tag{4}$$

$$\lambda_{n_2} - \lambda_{n_1} = p^q_{n_1 n_2} + \nu^q_{n_1 n_2}, \quad \forall q \in \mathcal{P}^+(n_1, n_2), \tag{5}$$

where $\mathcal{P}^+(n_1, n_2)$ is the set of paths from n_1 to n_2 for which there exists positive flow in the optimal market allocation. Equations (4) and (5) are fundamental no-arbitrage results for competitive markets. The pair of equations state that the price at node n_2 must be less than or equal to the price at node n_1 plus the marginal cost of transporting a unit from n_1 to n_2, with equality holding when there is positive flow from n_1 to n_2.

While equations (4) and (5) hold in general, there exist prices that satisfy these conditions that offer no meaningful insight into the relationship between nodal prices in the network. For example, consider a "star network" with a single producer directly connected to each consumer at zero cost. When consumers are not participating (i.e., $b_s = 0$) in the market, their equilibrium prices can be arbitrarily lower than the producer's equilibrium price. To eliminate such edge cases, we assume (without loss of generality) that all consumers participate in the market. Note that our focus going forward is on prices at the consumer nodes because the empirical "market price" of a commodity typically refers to the price for end consumers (e.g., price of retail gasoline or price of residential natural gas). Similarly, consumer prices are relevant for economists and policy-makers interested in consumer welfare. Thus, we make an assumption on participation of consumers.

ASSUMPTION 1. *We assume that* $b_s > 0 \ \forall s \in \mathcal{S}$ *in the optimal market allocation.*

Another way to interpret this assumption is that for every consumer, the welfare gained from the first infinitesimally small unit consumed will always exceed the cost of producing and transporting that unit. With this assumption, we can strengthen the equilibrium conditions (4) and (5).

LEMMA 1. *For every* $s \in \mathcal{S}$, $\lambda_s = \min\{\lambda_k + p^q_{ks} + \nu^q_{ks} \mid k \in \mathcal{K}_{(s)}, q \in \mathcal{P}_{(k,s)}\}$.

Lemma 1 states that the equilibrium price at a participating consumer node must be equal to the minimum marginal cost of production and transportation (including both explicit transportation costs and the shadow prices along the path) over the set of producer nodes to which the consumer is connected. When there is no congestion in the network, i.e., $f_{ij} < u_{ij} \ \forall (i,j) \in \mathcal{E}$, then $\nu_{ij} = 0 \ \forall (i,j) \in \mathcal{E}$ by equation (2e), and Lemma 1 can be further simplified as shown in Corollary 1.

COROLLARY 1. *For every* $s \in \mathcal{S}$, $\lambda_s = \min\{\lambda_k + p^*_{ks} \mid k \in \mathcal{K}_{(s)}\}$ *when* $f_{ij} < u_{ij}$, $\forall (i,j) \in \mathcal{E}$.

4. Price Integration in Networks

In this section, we study the relationship between equilibrium prices and the underlying transportation network. To isolate the effects of network topology, link costs, and capacity constraints on the distribution of prices, we consider markets with increasingly general transportation networks. Sections 4.1-4.3 study single market realizations with arbitrary demand and supply functions. In Section 4.4, we consider the implications of these results for the analysis of multiple market realizations when the transportation network is stable.

4.1. Uncapacitated networks without transportation costs

We first define a feature of the market topology that we term *structural integration*. A set of consumer nodes is structurally integrated if each node shares the same set of producers. If all consumer nodes in the network are structurally integrated, then we refer to the market as being structurally integrated.

DEFINITION 1. A set $\mathcal{S}_I \subseteq \mathcal{S}$ is *structurally integrated* if $\mathcal{K}_{(s)} = \mathcal{K}_{(r)}, \forall s, r \in \mathcal{S}_I$.

The main result in this subsection is that structural integration is a necessary and sufficient condition for the *law of one price* to hold in the absence of transportation frictions (i.e., $c_{ij} = 0$ and $u_{ij} = \infty$). The law of one price refers to a market having a single price for a common commodity irrespective of welfare and cost functions (Parsley and Wei 1996) and represents an extreme level of price integration. It is well known in the literature that in the absence of transportation frictions, the law of one price should theoretically hold for directly connected nodes. We extend this result to more general network topologies.

LEMMA 2. *Consider a market without transportation frictions: $c_{ij} = 0$ and $u_{ij} = \infty$ for all $(i, j) \in \mathcal{E}$. A set of consumers $\mathcal{S}_I$ will have common equilibrium prices ($\lambda_s = \lambda_r \ \forall s, r \in \mathcal{S}_I$), for all instantiations of welfare and cost functions if and only if the transportation network is structurally integrated ($\mathcal{K}_{(s)} = \mathcal{K}_{(r)}, \forall s, r \in \mathcal{S}_I$).*

The following example illustrates the difference between markets with and without structural integration.

Example 1 *Consider the network shown in Figure 1a. We assume that transportation costs are zero and there are no capacity constraints on the network. In this network, there exist instances where different producer cost functions can lead to different prices between the consumers. For example, suppose both consumers have the same welfare function $W_s(b) = b^{1/2}$, while the producers have different linear cost functions: $W_{k_1}(b) = b$ and $W_{k_2}(b) = 2b$. The equilibrium prices under this set of welfare functions are $\lambda_{s_1} = 1, \ \lambda_{s_2} = 2$, since consumer s_2 can only satisfy its demand from producer k_2, i.e., the more expensive producer.*

When we add links that connect k_1 to s_2, either directly (Figure 1b) or indirectly through s_1 (Figure 1c), the market becomes structurally integrated and consumer prices will be equal ($\lambda_{s_1} = \lambda_{s_2} = 1$).

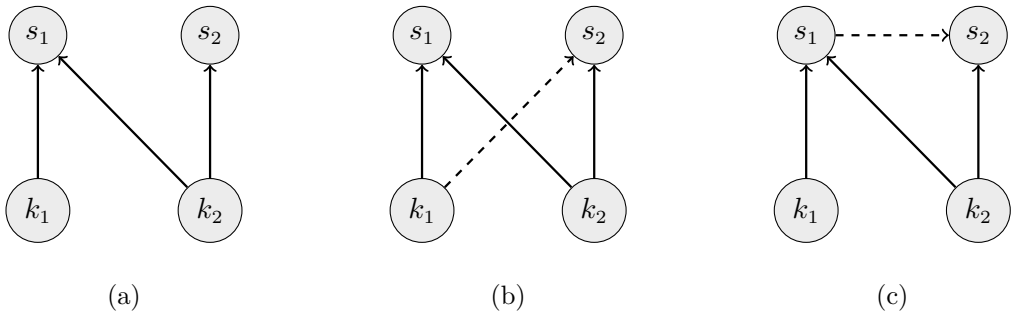

Figure 1 Examples of non-structurally integrated (a) and structurally integrated markets (b) and (c). Dashed lines indicate links which are not present in panel (a).

Structural integration implies that the set of consumers are connected to the same set of producers. Thus, in the absence of frictions impeding the movement of goods, the marginal price for all consumers will be the same. If the consumers are not structurally integrated, a producer who is connected to only a subset of consumers may sometimes have lower costs, resulting in lower prices for this subset of consumers.

Structural integration is important for differentiating price differences caused by transportation costs and capacity constraints from price differences due to the topology of the network. In the following sections where we examine richer transportation networks that include transportation costs and capacity constraints, we assume that the market is structurally integrated in order to isolate price effects that result from these network features.

REMARK 1. To ensure common market prices without structural integration, it suffices to assume that any set of producers that is accessible only by a strict subset of consumer nodes cannot produce enough to satisfy the demand of any of these nodes. This ensures that the full set of consumer nodes still competes over the same set of shared producer nodes for marginal supply, resulting in common prices.

4.2. Uncapacitated networks with transportation costs

Next, we consider markets where transportation costs are non-zero but links remain uncapacitated (i.e., $c_{ij} \geq 0$ and $u_{ij} = \infty$). This setting is representative of the majority of commodity market models in the literature. We show that in this setting, structural integration is necessary and sufficient to guarantee a well-defined neutral band, which we refer to as a *network neutral band*. Extending the pairwise neutral band to a network setting enables insight into price integration when consumers are not directly adjacent.

THEOREM 1. *Consider a market with an uncapacitated transportation network. A pair of consumer nodes $s, r \in \mathcal{S}$ are structurally integrated if and only if*

$$\min\{p^*_{ks} - p^*_{kr} \mid k \in \mathcal{K}_{(s)}\} \leq \lambda_s - \lambda_r \leq \max\{p^*_{ks} - p^*_{kr} \mid k \in \mathcal{K}_{(s)}\} \tag{6}$$

for all instantiations of welfare and cost functions.

When two consumer nodes are not structurally integrated, there exist welfare and cost functions that can generate arbitrarily large price differences. However, when two nodes are structurally integrated, the price difference is bounded and the bound is characterized entirely by the network structure and link costs. When the entire market is structurally integrated, the prices at any two consumer nodes are still related because they have access to the same set of producers, even though the cost to access the producers may vary. This is reflected in the key part that the differences

between shortest path distances to suppliers play in equation (6). Lemma 2, in the previous section, shows a special case of Theorem 1: since all transportation costs are zero, the shortest paths $p^*_{ks} = p^*_{kr}$ are also zero for all pairs of consumers so that equation (6) implies common prices. Next, we show that the bound in (6) is tight.

PROPOSITION 1. *Given any value Δ within the neutral band for a pair of structurally integrated consumers $s, r \in \mathcal{S}_I$, there exist welfare and cost functions for the market participants that will result in equilibrium prices λ_s, λ_r such that $\lambda_s - \lambda_r = \Delta$.*

Proposition 1 implies that the bound from the network neutral band, described in equation (6), will be at least as tight a bound on $\lambda_s - \lambda_r$ as the bound from the pairwise neutral band. Section B in the Appendix provides a simple example where the network neutral band is strictly tighter than the pairwise one. For convenience in our analysis and exposition, we will refer to the network neutral band as simply the neutral band. Furthermore, we define the mid-point and half-width of the neutral band between nodes r and s, ρ_{rs} and α_{rs}, as follows:

$$\rho_{rs} = \frac{1}{2}\left(\min\{p^*_{ks} - p^*_{kr} | k \in \mathcal{K}\} + \max\{p^*_{ks} - p^*_{kr} | k \in \mathcal{K}\}\right),$$
$$\alpha_{rs} = \frac{1}{2}\left(\max\{p^*_{ks} - p^*_{kr} | k \in \mathcal{K}\} - \min\{p^*_{ks} - p^*_{kr} | k \in \mathcal{K}\}\right).$$

The network neutral band can be used to illustrate the role of the "position" of producers in the network on the degree of price integration, which we explore in the following example.

Example 2 *This example explores the impact of producer proximity to consumers, measured by transportation costs, on the neutral band. Figure 2 shows three cases of two consumers supplied by three producers in a structurally integrated market.*

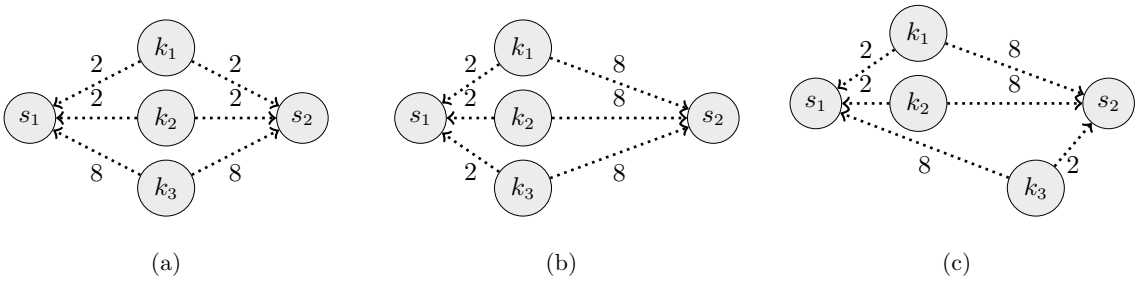

Figure 2 Three networks with different supplier-consumer transportation costs

In Figure 2a, both consumers face the same transportation costs from each producer. Thus, the half-width and midpoint of the neutral band is zero and the equilibrium prices for both consumers are always equal. In Figure 2b, s_1 faces lower transportation costs than node s_2, so the midpoint

is shifted and the equilibrium price at node s_1 will always be 6 units lower than s_2. In Figure 2c, each consumer can access a subset of producers with cheaper transportation costs. The neutral band midpoint is at zero but the half-width is 6. As a result, the absolute price difference between s_1 and s_2 can be up to 6 units but will vary depending on production costs.

This example provides insight into how the distribution of supply and demand over a market footprint can impact the neutral band, and, in turn, market integration. When demand is clustered together, shortest path costs from different producers will be similar for all consumers and might result in a situation as in Figure 2a. This results in a small neutral band centred around zero, which leads to a common market price for all consumers. When supply is clustered together, transportation costs for a consumer will be similar irrespective of the producer. This is the case in Figure 2b, which leads to a narrow neutral band, though the midpoint of the neutral band may be far from zero. This results in stable differences in consumer prices. The gasoline market studied in this paper features refining capacity clustered in the Gulf of Mexico region of the U.S. and is an example of this type of market. Finally, the implications for price integration are different in a market where producers are more dispersed with respect to consumers. In this case, certain suppliers will have lower transportation costs for certain consumers as is illustrated in Figure 2c. The resulting heterogeneous consumer preferences for suppliers leads to a wider neutral band within which demand and supply shocks may propagate throughout the market footprint leading to less integrated consumer prices.

4.3. Capacitated networks with transportation costs

We now allow links in the transportation network to be both costly and subject to capacity constraints (i.e., $c_{ij} \geq 0$ and $u_{ij} \leq \infty$). In this setting, positive shadow prices on capacity constraints can lead to a *congestion surcharge* borne by a subset of consumer nodes. Without capacity constraints, as described in Corollary 1, each consumer price will be equal to the minimum of the sum of the price at a producer node and the cost of transportation between the producer and consumer. We define the congestion surcharge as the part of the consumer price above this value:

Definition 2. The *congestion surcharge* w_s for a consumer node $s \in \mathcal{S}$ is the amount that the equilibrium price at s exceeds the uncapacitated delivery price to node s:

$$w_s = \max\{\lambda_s - \lambda_k - p^*_{ks} \mid k \in \mathcal{K}\}. \tag{7}$$

We can rearrange equation (7) to obtain

$$\lambda_s = \min\{\lambda_k + p^*_{ks} \mid k \in \mathcal{K}\} + w_s. \tag{8}$$

Corollary 1 shows that in the absence of capacity constraints, the congestion surcharge is zero. We will study the dynamics of these charges in driving apart equilibrium prices and creating local pricing discrepancies that would not otherwise exist.

Combining the result from Lemma 1 and equation (8), we can write w_s as

$$w_s = \min\{\lambda_k + p^q_{ks} + \nu^q_{ks} \mid k \in \mathcal{K}, q \in \mathcal{P}_{(k,s)}\} - \min\{\lambda_k + p^*_{ks} \mid k \in \mathcal{K}\}. \tag{9}$$

Equation (9) shows that w_s can be described as the difference between the cost of acquiring a unit when considering shadow prices in the network and and the cost when shadow prices are not considered. Using equation (9), we extend the neutral band described in Theorem 1 to the setting with capacity constraints:

THEOREM 2. *Let $r, s \in \mathcal{S}$. The price difference between r and s is bounded by*

$$\min\{p^*_{ks} - p^*_{kr} \mid k \in \mathcal{K}_{(s)}\} + w_s - w_r \leq \lambda_s - \lambda_r \leq \max\{p^*_{ks} - p^*_{kr} \mid k \in \mathcal{K}_{(s)}\} + w_s - w_r \tag{10}$$

over all welfare and cost functions.

Equation (10) shows that a pair of consumer nodes sharing the same congestion surcharge will have the same neutral band as in the setting with no capacity constraints. When the congestion surcharge differs between a pair of consumer nodes, the midpoint of the neutral band will be shifted. Notably, the width of the neutral band is not affected by the congestion surcharge. When there are no capacity constraints, $w_s = 0$ for all s (Corollary 1), equation (10) is equivalent to equation (6).

For the subsequent analysis of data, it is useful to assume the existence of a *root node* which is a consumer node with a congestion surcharge of zero. Using equation (10) we can derive a simple bound on each consumer price relative to the price of the root node $o \in \mathcal{S}$:

$$\min\{p^*_{ks} - p^*_{ko} \mid k \in \mathcal{K}_{(s)}\} + w_s + \lambda_o \leq \lambda_s \leq \max\{p^*_{ks} - p^*_{ko} \mid k \in \mathcal{K}_{(s)}\} + w_s + \lambda_o. \tag{11}$$

The windows for consumer prices described in the bounds in Equation (11) will be shifted both by the congestion surcharge from a congested link and by the price of the root node. It is convenient to think of the price of the root node as reflecting a broader market price for the commodity in the absence of capacity constraints. A corollary of equation (9) shows that such a node s will exist if there are no congested links on the path minimizing $\min\{\lambda_k + p^*_{ks} \mid k \in \mathcal{K}\}$. A sufficient condition for a node s to be a root node is thus that s is not downstream of any congested links. Root nodes are further discussed following Example 3.

4.3.1. Congestion on a single link. To best elucidate the relationship between market structure and the propagation of congestion surcharge throughout a network, we study the case where there is exactly one capacitated link in the network. We first consider price integration between the pair of nodes at either ends of this capacitated link.

PROPOSITION 2. *Consider a market where consumer nodes $i,j \in \mathcal{S}$ are joined by the link (i,j). If link (i,j) is the only congested link in the network, then $w_i = 0$ and $w_j = \nu_{ij}$.*

Proposition 2 is intuitive and states that when the flow on link (i,j) in a network reaches its capacity, node j incurs a congestion surcharge equal to the full shadow price of the link. Previous empirical literature has attempted to measure this congestion surcharge by examining price differences at either endpoints of a congested pipeline (Oliver et al. 2014). The more interesting case, which has not previously been characterized, is the impact of the capacitated link (i,j) on prices at nodes $s \in \mathcal{S}\backslash\{i,j\}$ that are not directly adjacent. We show that nodes which are not incident to the congested link can still incur a congestion surcharge, even when incoming flow into these nodes do not traverse the congested link. Furthermore, this surcharge is bounded above by the shadow price of the link.

We first require some additional formalization. Let $e \in \mathcal{E}$ denote the single congested link. Recall that p^*_{ks} is the cost of the minimum-cost path from k to s. Let $p^{*,\neg e}_{ks}$ be the cost of the minimum-cost "replacement" path from k to s which does not include link e and let $\delta_e(k,s) = p^{*,\neg e}_{ks} - p^*_{ks}$. The value $\delta_e(k,s)$ can be viewed as the maximum cost of continuing commerce between k and s in the absence of link e. If all paths from k to s include link e, then $\delta_e(k,s) := \infty$. Finally, let $\delta^{\min}_e(s) = \min\{\delta_e(k,s) \mid k \in \mathcal{K}\}$ and $\delta^{\max}_e(s) = \max\{\delta_e(k,s) \mid k \in \mathcal{K}\}$.

THEOREM 3. *Suppose there is a single congested link $e \in \mathcal{E}$ in the network with shadow price ν_e. Then, for all $s \in \mathcal{S}$,*

$$w_s \in [\min\{\nu_e, \delta^{\min}_e(s)\},\ \min\{\nu_e, \delta^{\max}_e(s)\}]. \tag{12}$$

Theorem 3 describes the trade-off required to use a replacement path for a congested link. In a network where that trade-off is high ($\delta^{\min}_e(s) > \nu_e$), it is less expensive to ship on link e and the congestion surcharge at node s reflects the full shadow price of link e, i.e., ν_e. However, when that tradeoff is small and it is relatively inexpensive to reroute the commodity to avoid link e ($\delta^{\max}_e(s) < \nu_e$), the congestion surcharge will be less than ν_e. The implications of the theorem are consistent with intuition on how network structure can mitigate costs of congestion. In a highly connected network, the cost of rerouting around a link (and by proxy $\delta^{\max}_e(s)$) is likely to be low, limiting the set of nodes whose price will reflect the full shadow price of a congested link. On the other hand, in a sparse network the cost of rerouting (and by proxy $\delta^{\min}_e(s)$) may be large, implying that the shadow price of a congested link can be fully reflected in many downstream nodes.

We use the following example to provide a comprehensive illustration of the relationship between network structure and pricing for three cases characterized by Theorem 3: a) the absence of any paths that avoid a congested link e ($\delta_e^{\min}(s) = \infty$), b) when all alternative paths have the same cost ($\delta_e^{\min}(s) = \delta_e^{\max}(s)$), and c) when alternative paths have different cost ($\delta_e^{\min}(s) < \delta_e^{\max}(s)$).

Example 3 *We examine outcomes for three markets illustrated in Figures 3a, 3b, and 3c. Each market features three consumer nodes, s_1, s_2 and s_3, and two producer nodes, k_1 and k_2. Each producer has the cost function $W_k(b_k) = b_k^2$ which possesses increasing marginal costs. The consumer's welfare functions are $W_s(b_{s_1}) = 10\sqrt{b_{s_1}}$, $W_s(b_{s_2}) = 20\sqrt{b_{s_2}}$, and $W_s(b_{s_3}) = 20\sqrt{b_{s_3}}$, which possess diminishing marginal utility.*

The markets differ only in the transportation network. Market 3a is connected by the illustrated network where all links have zero transportation costs and only link (s_1, s_2) (highlighted in red) has a capacity of 1 unit. Market 3b differs from market 3a by having the additional link (s_1, s_3) with a transportation cost of 1 unit. Market 3c differs from market 3a by having the additional link (k_1, s_3), also with a transportation cost of 1 unit. Figure 3 shows the equilibrium prices beside each node. Positive flows in the market allocation are shown by solid lines.

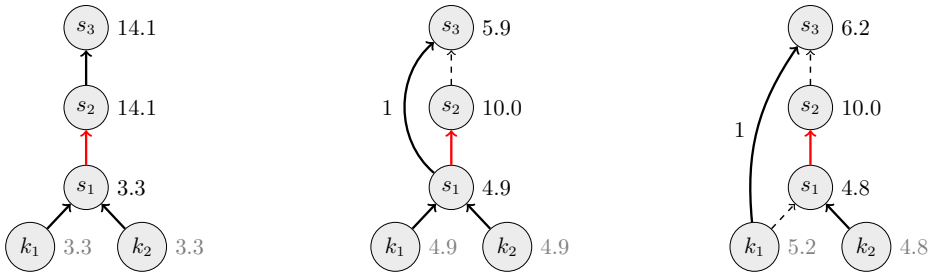

(a) $\delta_e^{\min}(s_3) = \infty$ (b) $\delta_e^{\min}(s_3) = \delta_e^{\max}(s_3) = 1$ (c) $\delta_e^{\min}(s_3) < \delta_e^{\max}(s_3)$

Figure 3 Equilibrium prices with a congested link (in red) in three different markets.

The shadow price for the link (s_1, s_2), denoted by ν_{s_1,s_2}, is equal to 10.8, 5.1, and 5.2 units respectively in markets 3a, 3b and 3c.

In Example 3, if the capacity constraint is removed, the equilibrium prices would be identical across all three markets and equal to 6.1 units, since all three markets are connected by the same subnetwork of zero cost paths. When link (s_1, s_2) has a capacity constraint which is reached, each market has a different set of equilibrium prices. Note that in each market, s_1 is a root node, since the minimum-cost paths from each producer to s_1 does not include link (s_1, s_2). Since the neutral band is zero for all consumer nodes, the price difference $\lambda_{s_2} - \lambda_{s_1}$ and $\lambda_{s_3} - \lambda_{s_1}$ directly reflect the congestion surcharge of the nodes s_2 and s_3, respectively. In all three markets, the equilibrium

price at s_2 is equal to the price at s_1 plus the shadow price of the link (s_1, s_2), which can be derived by observing that $\delta_e^{\min}(s_2) = \infty$ in equation (12). Practically, all flow to s_2 must come through s_1.

However, the options available for serving s_3 differs in the three markets. In market 3a, s_3 incurs the full shadow price of 10.8 units at equilibrium since, like node s_2, there do not exist any alternative paths for the commodity to reach s_3 ($\delta_e^{\min}(s_2) = \infty$). In markets 3b and 3c, there are alternative paths to s_3. In market 3b, the equilibrium price at node s_3 is 1 unit higher than at s_1, which can be explained by $\delta_e^{\min}(s_3) = \delta_e^{\max}(s_3) = 1$; any shadow price that exceeds one unit would result in flow being rerouted onto link (s_1, s_3), implying that the price difference between s_3 and s_1 would never exceed 1 unit. In market 3c, s_3 obtains all of the commodity from k_1 directly, with an equilibrium price that is 1.4 units higher than s_1. Since $\delta_e^{\min}(s_3) = 1, \delta_e^{\max}(s_3) = \infty$, equation (7) suggests that the congestion surcharge on node s_3 can be any value between 1 unit and the shadow price of 5.2 units, depending on the supply and demand functions.

Note that in the market 3c, the direct connection from k_1 to s_3 surprisingly results in s_3 incurring a higher price than it did in the market 3b. This outcome results from the fact that in market 3b, node s_3 could access both k_1 and k_2 cheaply, whereas s_3 can only access k_1 cheaply in market 3*c*. The more concentrated demand on k_1 in market 3c results in a higher production price at k_1 (due to the marginally increasing production cost), leading to a higher equilibrium price at s_3. Market 3c also highlights that examining only the direction of flows in a network may result in the misleading conclusion that s_3 is in a disjoint market from s_1, s_2. On the other hand, the equilibrium prices clearly highlight that both s_2 and s_3 do incur a positive congestion surcharge as a result of the congestion link, albeit different in magnitude.

Finally, note that if link (k_1, s_1) is the capacitated link, then the congestion surcharge cannot be fully observed in consumer prices because the shadow price of the congested link is applied to all consumers (i.e., $w_s > 0 \ \forall s \in \mathcal{S}$, and we do not observe the portion that is cancelled out by the $w_s - w_r$ term in equation (10)). Any market equilibrium will have a root node except in the case where a congested link is upstream of all consumer nodes; in such a setting, price differences exceeding the neutral band reflect an underestimate of the total surcharge.

4.4. Observations over multiple market realizations

Up to this point, we focused on the distribution of prices in a single market realization. We now extend our previous results to the case where we have multiple observations over a market. In particular, at each distinct "period", indexed by $t \in \mathcal{T} = \{1, \ldots, T\}$, we observe prices from an independent realization over a market with fixed network structure and link costs, although potentially different welfare functions, cost functions, and capacities. These dynamics are typical of energy markets where the transportation network is capital intensive and can be assumed to be static over

the medium term, whereas demand can shift quickly with consumer preferences (e.g., as a result of poor weather) while the network is prone to potential disruptions that can reduce link capacities.

PROPOSITION 3. *The set of equilibrium prices for $s \in \mathcal{S}$ over a market with fixed network structure and link costs can be expressed as*

$$\lambda_s^t = \eta^t + \rho_s + \epsilon_s^t + w_s^t, \quad \forall s \in \mathcal{S}, t \in \mathcal{T}, \tag{13}$$

where $\epsilon_s^t \in [-\alpha_s, \alpha_s]$ and $w_s^t \geq 0$.

Equation (13) highlights that the distribution of prices over a set of market realizations can be decomposed into a few different components which vary over time, nodes or both (as indexed). More specifically, the set of prices can be decomposed into a node-invariant "market trend" η^t, a set of time invariant terms ρ_s and α_s representing the network neutral band bounding the idiosyncratic movement of ϵ_s^t, and a term w_s^t representing the congestion surcharge. Note that since the ϵ_s^t is bounded by the time invariant terms, the term w_s^t is the only term that can be unconstrained both spatially (i.e., per node) and temporally (i.e., per $t \in \mathcal{T}$).

When there are no binding capacity constraints in the network over the set of periods $\mathcal{T}$, i.e., $w_s^t = 0, \ \forall s \in \mathcal{S}, t \in \mathcal{T}$, changes in the participant's welfare and cost functions between market realizations will determine the value of ϵ_s^t within the bound $[-\alpha_s, \alpha_s]$. Price shocks generated from mild local demand and supply shifts are likely to be contained within the neutral band without affecting the overall market, whereas sufficiently large local demand or supply shocks will shift prices throughout the market by changing the value of η^t. In the setting where there are binding capacity constraints, the additional terms w_s^t reflect the congestion surcharge experienced by different nodes in the market. Depending on the network configuration, it is possible that large price shocks generated from significant local demand changes can remain locally contained, i.e., w_s^t will be positive for a small subset of nodes without changing η^t.

5. Estimating the Congestion Surcharge from Pricing Data

In this section, we present a framework for estimating the congestion surcharges at different nodes from observed pricing data.

5.1. Surcharge Estimation Model

The surcharge estimation model (SEM) is based on the price decomposition shown in equation (13). It takes as input a set of spatial prices $\boldsymbol{\lambda} = \{\lambda_s^t\}_{s \in \mathcal{S}, t \in \mathcal{T}}$ and a set of user-selected parameters

and outputs an estimate of the congestion surcharge at each node over the given time horizon. In its most generic form, the SEM model can be presented as follows:

$$\underset{\eta^t,\rho_s,\epsilon_s^t,w_s^t,\alpha_s}{\text{minimize}} \quad \sum_{s\in\mathcal{S}} \alpha_s \tag{14a}$$

$$\text{subject to} \quad \lambda_s^t = \eta^t + \rho_s + \epsilon_s^t + w_s^t, \quad \forall s \in \mathcal{S}, t \in \mathcal{T}, \tag{14b}$$

$$|\epsilon_s^t| \leq \alpha_s, \quad \forall s \in \mathcal{S}, t \in \mathcal{T}, \tag{14c}$$

$$w_s^t \in \mathcal{W}, \ \forall s \in \mathcal{S}, t \in \mathcal{T}. \tag{14d}$$

Constraints (14b) and (14c) are derived directly from the price decomposition presented in equation (13). The variables η^t capture a node-invariant underlying trend, while the variables ρ_s, ϵ_s^t and α_s capture the time-invariant neutral bands. All remaining price variation is captured by the variables w_s^t, representing congestion surcharges. Constraints on w_s^t are represented by $\mathcal{W} \subseteq \mathbb{R}^+$.

If price movements are perfectly synchronized across all nodes, i.e., price differences are constant, the optimal objective value will be zero and the prices λ_s^t can be entirely explained by the node-invariant term η^t and time-invariant term ρ_s. The variables ϵ_s^t and w_s^t capture deviations from price integration, which are attributed to variation within the neutral band and transient congestion in the transportation links, respectively. While model (14) is derived directly from the price decomposition, the model without any additional constraints in the form of $\mathcal{W}$ is underdetermined, as shown by the following remark.

Remark 2. If $\mathcal{W} = \mathbb{R}^+$, the optimal objective value of (14) will always be zero.

When w_s^t is unconstrained, there is a free variable w_s^t for every price λ_s^t, and an optimal solution would simply be to set $w_s^t = \lambda_s^t$ (assuming all λ_s^t are positive) and all other variables to zero. This solution reflects the hypothesis that there is congestion at every time period across all nodes. However, congestion events are expected to be transient and should not be present for large proportions of the time horizon. The other extreme solution is setting $\mathcal{W} = \{0\}$, which represents the hypothesis that nodes do not incur congestion surcharges over the observed period and all price variations can be explained fully through changes in supply and demand. A judicious choice of $\mathcal{W}$ can be used to more finely differentiate between these two extreme explanations for non-integrated prices, and the strategies to do so are discussed in detail in the following subsection.

5.2. Approach to congestion surcharge identification

Our identification strategy is based on: 1) limiting the proportion of periods that the congestion surcharges may be active; 2) resolving precise values for the congestion surcharges using a conservative strategy; 3) determining the proportion of congested periods in a principled manner. This subsection addresses these points in turn.

5.2.1. Identifying periods of congestion. We include a set of *time-limiting constraints* to force $w_s^t = 0$ for a fraction of total time periods, while allowing the precise set of periods to be selected by the model. Let $\beta \in [0,1]$ define a parameter representing a fraction of the time horizon for which w_s^t is unconstrained, with $w_s^t = 0$ for all other time periods. The time-limiting constraints can be written as

$$w_s^t \leq \psi^t M,\ \sum_{t \in \mathcal{T}} \psi^t \leq \lfloor \beta T \rfloor,\ \psi^t \in \{0,1\}, \quad \forall s \in \mathcal{S},\ t \in \mathcal{T}. \tag{15}$$

The binary variables ψ^t determine periods for which the congestion surcharge is free ($\psi^t = 1$) or fixed to zero ($\psi^t = 0$), and M represents a sufficiently large value such that w_s^t will never reach its upper bound when $\psi^t = 1$. The parameter β represents an estimate of the fraction of time periods for which the underlying network is congested. The $\lceil (1-\beta)T \rceil$ periods identified as uncongested ($\psi^t = 0$) are used to fit the variables ρ_s such that we can use precisely these parameters to estimate w_s^t over periods where $\psi^t = 1$.

5.2.2. Identifying congestion surcharge values. Next, we introduce a set of *conservative-estimation* constraints that we use to remove one degree of freedom from the variable estimates. First, we note that if (ϵ_s^t, w_s^t) represents a pair of solutions to the SEM where t is a period for which w_s^t is free, it is possible to modify the solution to $(\epsilon_s^t - \delta, w_s^t + \delta)$ without changing the objective value. The range of possible values of w_s^t for which the solution remains optimal is potentially large ($\delta \in [-\alpha_s + \epsilon_s^t, \alpha_s + \epsilon_s^t]$). To handle this ambiguity, we enforce conservative estimates of the surcharges w_s^t, and capture only surcharges resulting in price movements that exceed the neutral band. So, w_s^t will only capture parts of the price that strictly exceed α_s. This is enforced using the following constraints:

$$w_s^t \leq \pi_s^t M,\ \epsilon_s^t + (1-\pi_s^t)M \geq \alpha_s,\ \pi_s^t \in \{0,1\}, \quad \forall s \in \mathcal{S}, t \in \mathcal{T}. \tag{16}$$

Identification issues also exist between w_s^t and η^t during congested periods. In particular, without impacting the optimality of a solution, we can make the values of w_s^t arbitrarily larger by shifting value from η^t. That is, $(\epsilon_s^t + w_s^t + \delta, \eta^t - \delta)$ is also a solution for any $\delta \geq 0$, since the negative and positive δ values will cancel each other out. We rectify this problem by adding a constraint to select the maximal value of η^t from the set of optimal solutions, leading to the minimal estimate of w_s^t. This is enforced with the following set of constraints,

$$\sum_s \gamma_s^t \geq \psi^t,\ \epsilon_s^t \leq -\alpha_s + (1-\gamma_s^t)M, \quad \forall s \in \mathcal{S}, t \in \mathcal{T}, \tag{17}$$

forcing $\epsilon_s^t = -\alpha_s^t$ for at least one s in each period $t \in \mathcal{T}$ for which $\psi^t = 1$. These constraints ensure that η^t (w_s^t) is the largest (smallest) possible value out of the set of optimal solutions.

5.2.3. Complete mixed-integer linear optimization formulation. We now formulate the SEM as a mixed-integer linear optimization model, where all pricing data is represented by λ_s^t:

$$
\begin{aligned}
z(\beta) := \text{ minimize } & \sum_{s\in\mathcal{S}} \alpha_s && \text{(18a)}\\
\text{subject to } & \lambda_s^t = \eta^t + \rho_s + \epsilon_s^t + w_s^t, \quad \forall s\in\mathcal{S}, t\in\mathcal{T}, && \text{(18b)}\\
& \epsilon_s^t \geq -\alpha_s, \quad \forall s\in\mathcal{S}, t\in\mathcal{T}, && \text{(18c)}\\
& \epsilon_s^t \leq \alpha_s, \quad \forall s\in\mathcal{S}, t\in\mathcal{T}, && \text{(18d)}\\
& w_s^t \leq \psi^t M, \quad \forall s\in\mathcal{S}, t\in\mathcal{T}, && \text{(18e)}\\
& \sum_{t\in\mathcal{T}} \psi^t \leq \lfloor \beta T \rfloor, && \text{(18f)}\\
& w_s^t \leq \pi_s^t M, \quad \forall s\in\mathcal{S}, t\in\mathcal{T}, && \text{(18g)}\\
& \epsilon_s^t + (1-\pi_s^t)M \geq \alpha_s, \forall s\in\mathcal{S}, t\in\mathcal{T}, && \text{(18h)}\\
& \sum_{s} \gamma_s^t \geq \psi^t, \quad \forall t\in\mathcal{T}, && \text{(18i)}\\
& \epsilon_s^t \leq -\alpha_s + (1-\gamma_s^t)M, \quad \forall s\in\mathcal{S}, t\in\mathcal{T}, && \text{(18j)}\\
& \gamma_s^t, \psi^t, \pi_s^t \in \{0,1\}, \quad \forall s\in\mathcal{S}, t\in\mathcal{T}, && \text{(18k)}\\
& w_s^t \geq 0 \quad \forall s\in\mathcal{S}, t\in\mathcal{T}. && \text{(18l)}
\end{aligned}
$$

Constraints (18e) and (18f) define the time-limiting constraints, and constraints (18g)-(18j) define the conservative-estimation constraints. It suffices to set $M = \max\{\lambda_r^t - \lambda_s^t \mid r,s\in\mathcal{S},\ t\in\mathcal{T}\}$, which is the largest absolute price difference between any two nodes across the entire time horizon.

A simpler reformulation. Finally, we show that model (18) can be simplified by introducing a new variable $\bar{w}_s^t := w_s^t + \epsilon_s^t - \alpha_s$. With this new variable, constraints (18b) and (18c) can be rewritten as

$$
\begin{aligned}
& \lambda_s^t = \eta^t + \rho_s + \alpha_s + \bar{w}_s^t, \quad \forall s\in\mathcal{S}, t\in\mathcal{T}, && \text{(19a)}\\
& \bar{w}_s^t \geq -2\alpha_s, \quad \forall s\in\mathcal{S}, t\in\mathcal{T}. && \text{(19b)}
\end{aligned}
$$

In this new representation, the neutral bands in the absence of congestion are defined as bands of $\bar{w}_s^t \in [-2\alpha_s, 0]$ around mid-points $-\alpha_s$. Since $w_s^t \geq 0$ and $\epsilon_s^t - \alpha_s \leq 0$, then $\bar{w}_s^t > 0$ if and only if $w_s^t > 0$, which implies that constraints (18e) and (18f) can be equivalently defined on $\bar{w}_s^t$.

Constraints (18d), (18g) and (18h) in model (18) ensure that the variable w_s^t can only be positive if $(w_s^t + \epsilon_s^t)$ exceeds the neutral band. These constraints are no longer necessary in the new representation; when $\bar{w}_s^t > 0$, it by definition representing the setting in which the neutral band has been

exceeded. In other words, when both ϵ_s^t and w_s^t appear in constraint (18b), we could add constants with opposite signs to each variable while retaining the objective value, and the constraints were added to avoid this setting. When we combine these two variables in $\bar{w}_s^t$, this issue is resolved. As a result, constraints (18g) and (18h) can be removed entirely and the set of binary variables π_s^t that appear only in these constraints can also be removed.

$$\underset{\eta^t,\rho_s,\alpha_s,\bar{w}_s^t,\psi^t,\gamma_s^t}{\text{minimize}} \quad \sum_{s\in\mathcal{S}} \alpha_s \tag{20a}$$

$$\text{subject to} \quad \lambda_s^t = \eta^t + \rho_s + \alpha_s + \bar{w}_s^t, \quad \forall s \in \mathcal{S}, t \in \mathcal{T}, \tag{20b}$$

$$\bar{w}_s^t \geq -2\alpha_s, \quad \forall s \in \mathcal{S}, t \in \mathcal{T}, \tag{20c}$$

$$\bar{w}_s^t \leq \psi^t M, \quad \forall s \in \mathcal{S}, t \in \mathcal{T}, \tag{20d}$$

$$\sum_{t\in\mathcal{T}} \psi^t \leq \lfloor \beta T \rfloor, \tag{20e}$$

$$\bar{w}_s^t \leq -2\alpha_s + (1-\gamma_s^t)M, \quad \forall s \in \mathcal{S}, t \in \mathcal{T}, \tag{20f}$$

$$\sum_{s} \gamma_s^t \geq \psi^t, \quad \forall t \in \mathcal{T}, \tag{20g}$$

$$\gamma_s^t, \psi^t \in \{0,1\}, \quad \forall t \in \mathcal{T}. \tag{20h}$$

Given optimal values of $\bar{w}_s^t$ from model (20), we can calculate values of the original w_s^t and ϵ_s^t variables as follows. If $\bar{w}_s^t \geq 0$, then $w_s^t = \bar{w}_s^t$ and $\epsilon_s^t = \alpha_s$. If $\bar{w}_s^t < 0$, then $w_s^t = 0$ and $\epsilon_s^t = \bar{w}_s^t + \alpha_s$.

Computation over large datasets. A potential complication may arise when solving model (20) over large datasets. Since model (20) does not explicitly account for the sequential nature of time periods and instead treats each $t \in \mathcal{T}$ independently, model (20) includes the problem of choosing the best βT independent time periods out of $\mathcal{T}$. The solution space of this problem can be particularly large when the number of time periods T is large and β is close to 0.5. We propose a set of (optional) constraints to reduce the complexity of solving the SEM over large datasets. For a fixed $t \in \mathcal{T}$ and positive integer m, let $T_{ub}(t,m) = \min\{T, t+m\}$ and $T_{lb}(t,m) = \max\{0, t-m\}$. We can add the following set of constraints to the model:

$$\sum_{t^*=t}^{T_{ub}(t,m)} \psi^{t^*} \geq \nu^t \cdot (T - T_{ub}(t,m) + 1), \quad \forall t \in \mathcal{T}, \tag{21a}$$

$$\psi^t \leq \sum_{t^*=T_{lb}(t,m)}^{t} \nu^{t^*}, \quad \forall t \in \mathcal{T}, \tag{21b}$$

$$\nu^t \in \{0,1\}, \quad \forall t \in \mathcal{T}. \tag{21c}$$

These constraints explicitly link adjacent time periods by enforcing the following condition: a period t can be selected by the SEM, i.e., $\psi^t = 1$, if and only if a *block* of adjacent time periods, including t, of minimum size m is selected. Large datasets by definition are highly granular (e.g.,

daily prices over an extended period of time). Thus, the addition of constraints (21a)-(21c) when solving the SEM with large datasets reflect the observation that empirically, network congestion events are unlikely to appear and resolve instantaneously (e.g., within a single day), but are instead more likely to persist across several adjacent time periods (e.g., across several days).

5.3. Exploring market characteristics with β

The β parameter determines the proportion of time periods where the surcharge terms w_s^t can take positive values. In practice, this parameter determines the tendency of the algorithm to classify pricing deviations as those caused by capacity constraints ($w_s^t > 0$) and those caused by idiosynchratic changes in supply and demand ($w_s^t = 0$). Increasing β corresponds to increasing the algorithms sensitivity to the effects of capacity constraints. If β is set too low, the algorithm may not be able to fully identify the price movements associated with capacity constraints, and if it is set too high it may misclassify idyosyncratic demand shocks. This challenge is analogous to problems in unsupervised learning such as determining the correct number of clusters in k-means clustering. Our approach is to use complementary methods to ensure that the results, in particular the collection of estimated pricing deviations, are consistent with expected characteristics of capacity bottlenecks.

Manual examination. We examine the congestion surcharge estimates over different β values. Bottlenecks in the underlying network are likely to manifest as price increases over contiguous locations and adjacent time periods. On the other hand, we have low confidence over low magnitude, surcharge estimates that are heterogenously dispersed geographically and temporally. By increasing the values of β, we can examine the surcharge estimates to identify thresholds for which further increases in β result in more frequent appearance of surcharge estimates exhibiting qualities for which we have low confidence. We elaborate further using empirical data in Section 6.

Changes in model metrics. To improve our understanding of where capacity constraints are active, we consider how the objective value $z(\beta)$ and the total surcharge $\sum_s \sum_t w_s^t$ vary as β increases. The objective value corresponds to an estimation of the total idiosyncratic pricing deviations and the total surcharge corresponds to the fit of the prices with respect to the neutral band. Examining these metrics for "elbows", points where the rate of change of the metric exhibits a discrete sustained change, allows us to pinpoint levels of β where any new detected events have distinctly different characteristics. This method is analogous to the practice in k-means clustering of examining changes in within-cluster variation to identify the correct measure of clusters as k is increased.

Examining the change in objective value $z(\beta)$ as β increases shows the degree to which newly identified capacity events substitute for unexplained pricing variation. As changes in $z(\beta)$ slow down with respect to β, the value of increasing β at explaining pricing variation in the dataset

also slows. Examining the change in the total surcharge as β increases provides an indication of the magnitude and duration of the pricing effects of newly identified capacity events. Prices which exceed the neutral band significantly over a sustained period of time, such that $\sum_s \sum_t w_s^t$ is large, are more likely to be a signal of irregularities in the underlying market. On the other hand, if prices only exceed the neutral band sightly and are short-lived, such that $\sum_s \sum_t w_s^t$ is small, then the confidence we have on w_s^t being congestion surcharge rather than noise is low. Discrete changes in the rate of total surcharge increase indicates transitions between such phenomena.

6. Case study: The Southeastern U.S. Gasoline Market

In this section, we present a case study on the southeastern U.S. gasoline market and demonstrate the effectiveness of our surcharge estimation method in capturing the effect of major network disruptions on gasoline prices. Extensive government deregulation on the supply side and price transparency on the demand side have made the gasoline market one of the most competitive commodity markets in the U.S. (Paul et al. 2001, Holmes et al. 2013). Thus, the gasoline market fits well into the market model we have proposed. This market, like the natural gas market, relies on highly specialized pipeline infrastructure to facilitate trade and competition between different market participants.

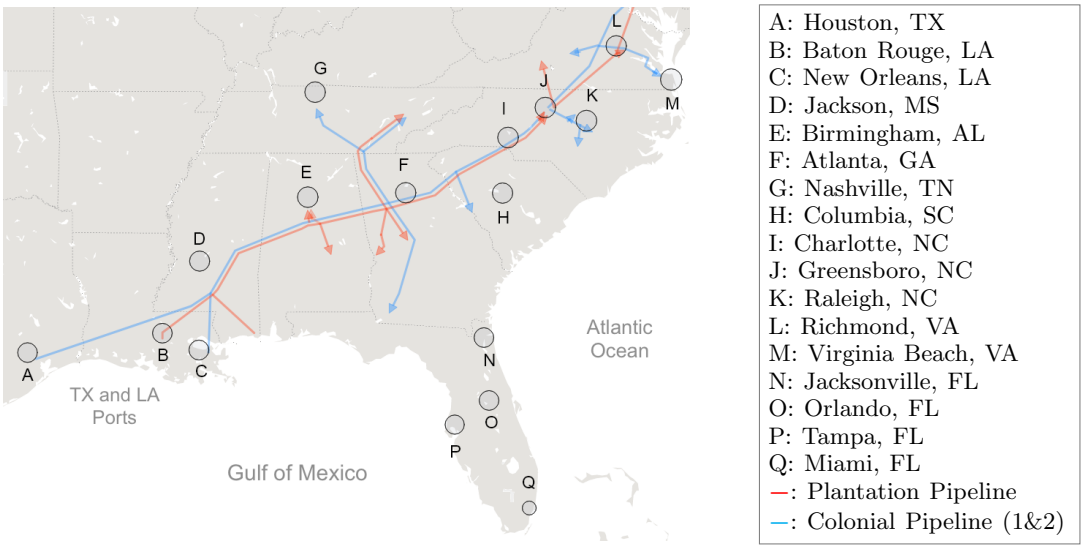

Figure 4 The pipeline network and the cities considered in this study.

6.1. Market and data description

The region that we consider, shown in Figure 4, spans from Texas to Virginia and has substantial refining, transportation and consumption activities. Over 50% of the United States' refining capacity is located along the coast of Texas and Louisiana. The refineries feed into two main pipelines,

the Colonial Pipeline (in blue) and the Plantation Pipeline (in red), which transport gasoline to the southeastern and eastern states of the U.S. The cities in Southern Florida on the other hand are serviced by tankers delivering gasoline from ports in Texas and Louisiana. The fact that the southeastern market is serviced almost exclusively by these refineries, coupled with the close proximity of refineries to each other, suggests that strong price integration should be expected in the absence of capacity constraints.

We obtained daily gasoline prices of the seventeen cities marked in Figure 4 from January 1, 2016 to December 31, 2017. The cities chosen include some of the most populated cities in the region. Daily prices are calculated from the last daily price of regular gasoline at all gasoline stations within the United States Postal Service (USPS) designated boundaries of the city. This data was collected through a combination of fleet card transactions, crowd-sourcing and direct retail pricing, and acquired from a data aggregator. A set of summary statistics for the data is found in Table 1 in the Electronic Companion. Finally, since federal and state motor fuel taxes are typically updated on the first day of each year (EIA 2019), we split our data into two sets, one per year. Having two sets of data also offers two instances with which to test the methodology.

6.2. Setup and preliminary results

We begin by analyzing the estimated market characteristics over different β values. To ensure that the SEM can be solved to optimality within an appropriate time window, in this case a few hours, we consider the SEM with the addition of constraints (21a)-(21c) with $m = 7$, corresponding to identifying blocks of adjacent time periods that are a week or more in duration. For each year, the SEM is solved with $\beta = \{0, 0.01, 0.02, ...0.30\}$.

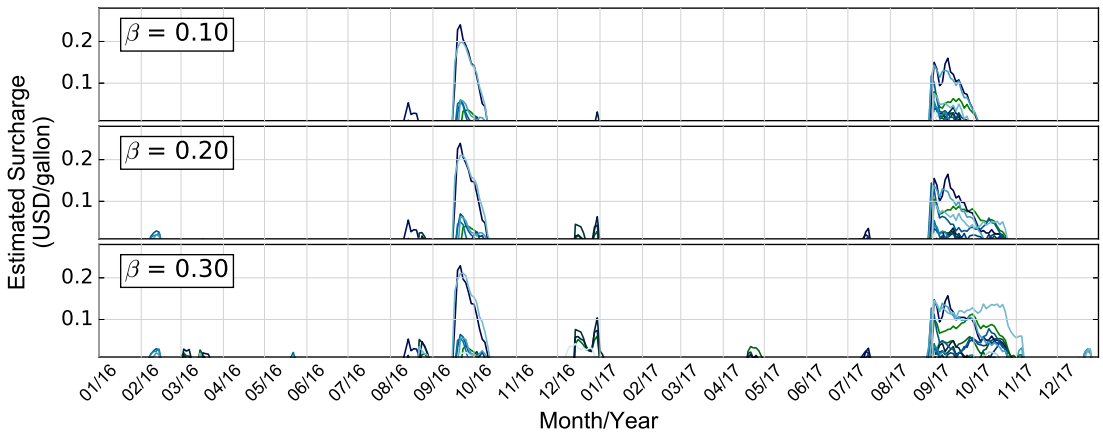

Figure 5 Estimated congestion surcharge in 2016 and 2017 over different β values.

Figure 5 shows a snapshot of the estimated congestion surcharge values over $\beta = \{0.10, 0.20, 0.30\}$. While the locations are not labeled in this figure, the figure highlights the the magnitude, trajectory and persistence of estimated surcharge values over increasing β values. Figure 6 shows the metrics proposed in Section 5.3; the objective value and the total surcharge over different β values are shown in Figures 6a and 6b whereas the change in these values are shown in Figures 6c and 6d. For ease of exposition, we use β_{2016} and β_{2017} when referring specifically to the 2016 and 2017 dataset.

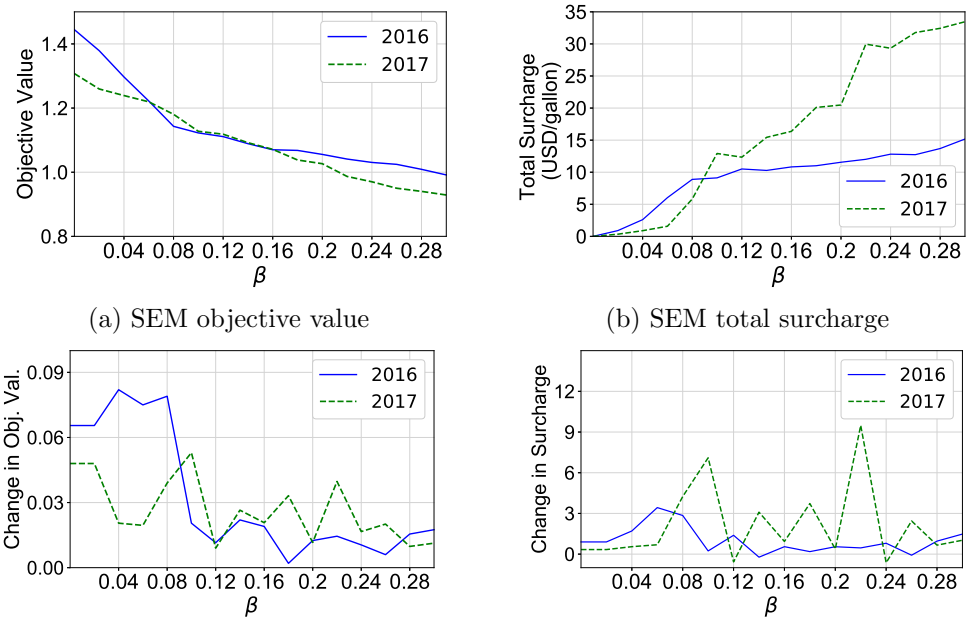

(a) SEM objective value

(b) SEM total surcharge

(c) Change in objective value

(d) Change in total surcharge

Figure 6 The calibration metrics over different β values.

For the year 2016, we observe a distinct change in both the rate of total surcharge increase and the rate of objective value decrease at $\beta_{2016} = 0.08$, as seen in Figures 6c and 6d. Empirically, this β_{2016} value marks a threshold at which point a distinct "cluster" of surcharge estimates is found. The surcharge estimates in this cluster, shown in Figure 5 to span several weeks during the months of September and October of 2016, are large in magnitude and contiguous both geographically and temporally. For the year 2017, we observe a distinct change in the rate of total surcharge increase, this time at $\beta_{2017} = 0.1$ and $\beta_{2017} = 0.22$ as shown in Figure 6d. Empirically, $\beta_{2017} = 0.22$ again marks a threshold at which point we capture a cluster of surcharge estimates that are large in magnitude and contiguous, shown in Figure 5 to be during the months of September - November 2017. Surcharge estimates that appear with β values exceeding these thresholds are lower in magnitude and occur over more dispersed time periods.

The two periods of time over which we detect significant congestion surcharge, namely September - October 2016 and September - November 2017, coincide with periods of severe weather events and network disruptions. On the other hand, surcharge estimates found over other time periods are relatively lower in magnitude and exhibit features that are consistent with congestion events during normal market operations. Since we cannot validate these smaller events from secondary sources, for the remainder of this section, we focus on studying gasoline price dispersion over the two time periods with well-documented market disruptions, using the estimated congestion surcharge values (obtained with $\beta_{2016} = 0.08$ and $\beta_{2017} = 0.22$) along with publicly available data of the pipeline system.

6.3. Study I: Price shocks from 2016 pipeline disruption

On September 9, 2016, a major pipeline leak was discovered on Line 1 of the Colonial Pipeline in Shelby County (see Figure 7), and a partial shutdown of that segment of the pipeline immediately followed (ICF 2016). The shutdown lasted until September 21, when the pipeline resumed full operating capacity. On October 31, 2016, a deadly pipeline explosion in Shelby County caused a partial shutdown of the pipeline, and operations were restarted on November 8. These dates are shaded in the inset of Figure 7.

The inset of Figure 7 shows the trajectory of the congestion surcharge for cities that experienced significant surcharges immediately following the pipeline leak. Consistent with our theory, these cities are all downstream from the leak. The map in Figure 7 shows the *cumulative* congestion surcharge (area under the curves in the inset) for each city in the region. First, we note that there is a lag between when the first disruption occurs and when the surcharge is observed. This observation captures the effects of the use of stored inventory, well-documented around this period (EIA 2016b), to mitigate potential price shocks. Second, we note that the congestion surcharge over all locations begins to decrease immediately after the pipeline is restored. However, it takes three full weeks for the price differences to completely disappear, highlighting the effects of high demand for pipeline capacity (to replenish inventories) following the disruption. Interestingly, we do not identify any congestion surcharge associated with the second disruption, which is likely due to a restocking of inventories to much higher levels following the previous disruption (EIA 2016a).

We observe that the locations immediately downstream of the site of disruption, in particular, Atlanta (label F) and Nashville (label G), observed the most significant price increases. Furthermore, it is easy to observe, especially in the case of Nashville, that there are no alternative sources of pipeline transportation other than the Colonial Pipeline. Interestingly, we find that all estimated surcharge values are roughly bounded from above by the surcharge incurred at Atlanta, which is the first downstream node of the disrupted pipeline that could not be easily supplied by other

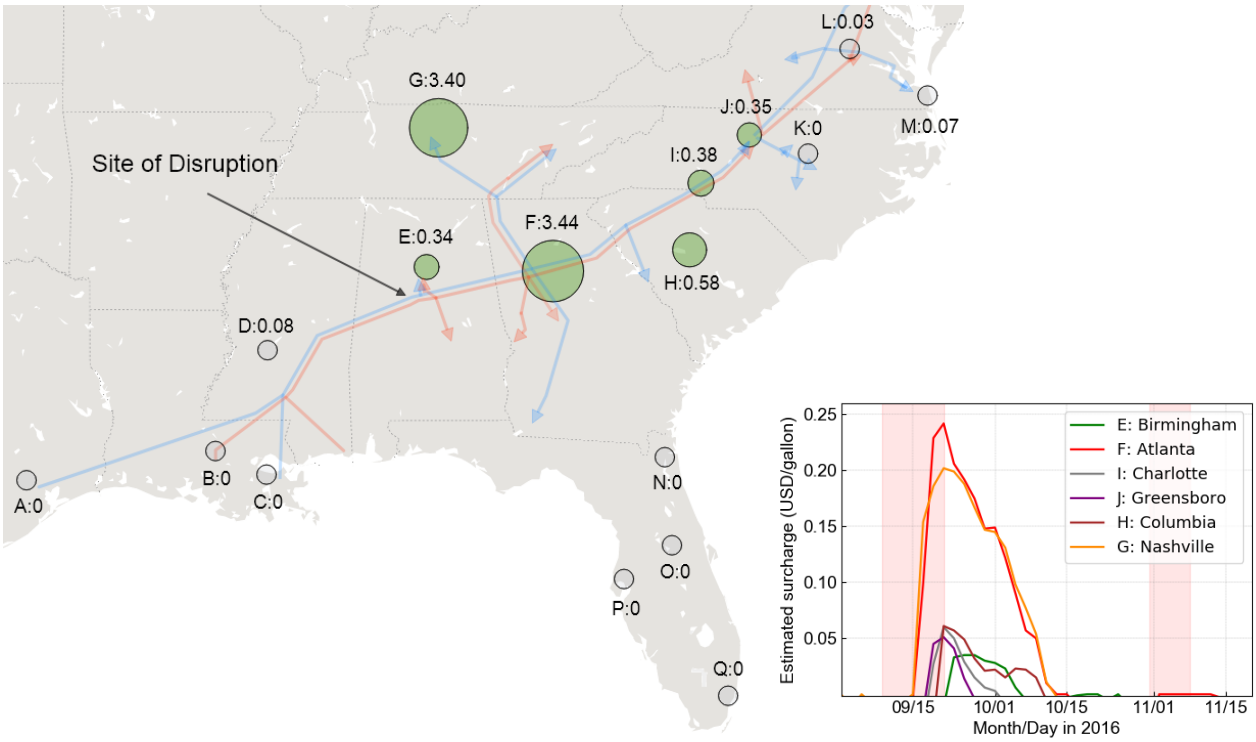

Figure 7 Map: cumulative estimated surcharges (with $\beta = 0.08$) resulting from 2016 pipeline disruption. Inset: estimated per-period surcharge from September to November 2016.

means of short-haul transportation such as trucks. This is consistent with our theoretical analysis, namely Theorem 3 and Example 3, which show that in a setting with a single disrupted link: 1) the location most directly downstream of the link incurs the most significant surcharge, equal to the shadow price of the link and 2) other locations will incur a surcharge bounded by this shadow price, with the magnitude dependent on the availability of alternative transportation resources.

The effect of alternative transportation resources is further highlighted by noting that the estimated surcharge values in the cities immediately downstream of Greensboro (label J), which serves as a major junction point where the pipelines can unload their supply, are essentially negligible. During the pipeline disruption, which occurred in Line 1 of the Colonial Pipeline, a second pipeline running in parallel (Line 2) that is typically used to transport heating oil, diesel and jet fuel, was temporarily used to transport gasoline to the eastern cities (EIA 2016b). The low levels of estimated surcharge in the cities downstream of Greensboro provide strong evidence that this rerouting of gasoline (on Line 2) and the existence of other transportation resources (the Plantation Pipeline) is crucial in mitigating price increases during network disruptions.

Finally, we note that congestion surcharge was not identified in any of the cities in Florida. This is consistent with what we would expect, since gasoline is delivered to these cities through tankers rather than by the Colonial and Plantation pipeline network.

6.4. Study II: Price shocks from 2017 hurricane season

The southeastern U.S. witnessed a catastrophic hurricane season in the fall of 2017. Most notable were Hurricanes Harvey and Irma, which together caused nearly $200 billion dollars worth of damage in this region alone. These two hurricanes also created large disruptions and logistical challenges in the petroleum supply chain. Hurricane Harvey, which made landfall in Texas and Louisiana during the last week of August 2017, resulted in the closure of refineries, docking of tankers, and the Colonial Pipeline being shut down on August 30 for one week, resuming operations at limited capacity on September 6 (EIA 2017a). Immediately following Harvey, Hurricane Irma, traveling from the Caribbean up to Florida, forced ports in Florida to close in the first two weeks of September. The reduced operations at ports around Texas, Louisiana and Florida resulted in significantly reduced product delivery to Florida during the hurricane season, lasting approximately from August 25 to September 13 (EIA 2017b).

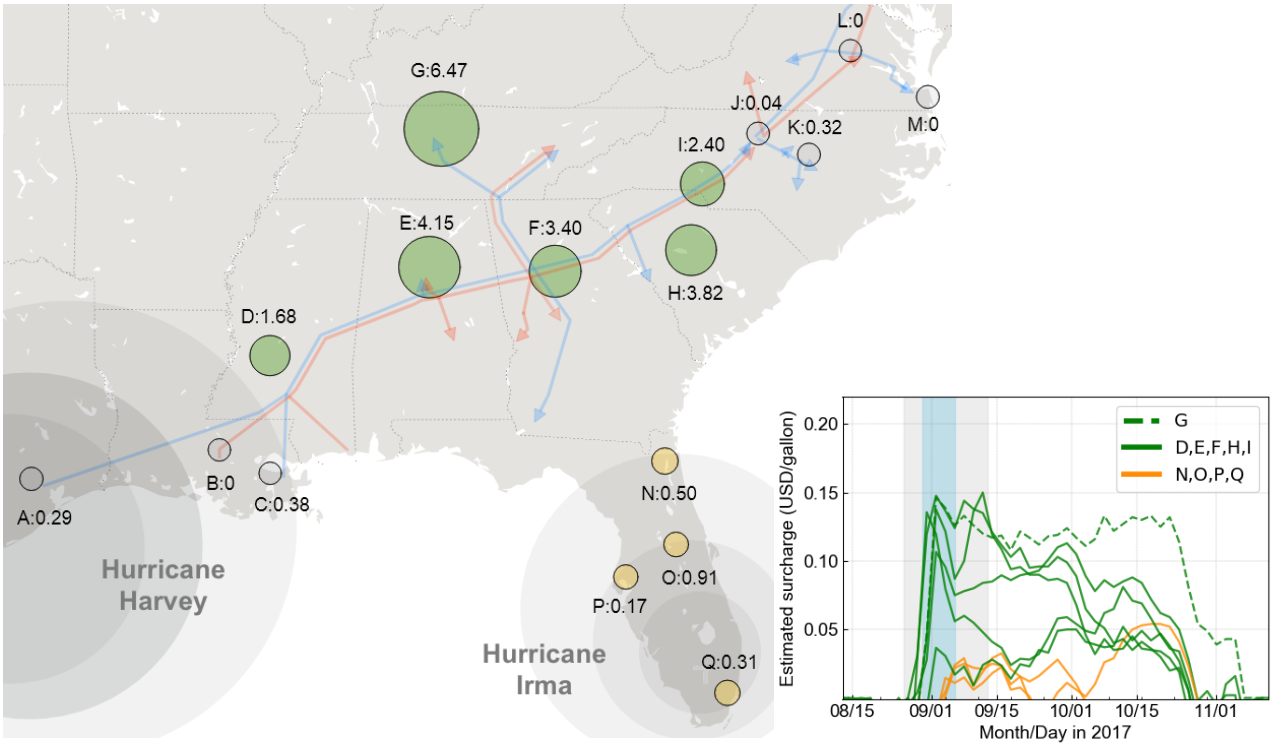

Figure 8 Map: cumulative estimated surcharges (with $\beta = 0.22$) resulting from 2017 hurricane season. Inset: estimated per-period surcharge from August to November 2017. The time periods for the Colonial Pipeline closure (Aug. 30th to Sept. 6th) is highlighted in blue and that of port closures (Aug. 25th to Sept. 13th) is highlighted in gray.

First, we find that the estimated surcharge values of the cities labeled D, E, G, F, H, I (and highlighted in green) coincide with and spike immediately following the closure of the Colonial Pipeline.

These cities lie directly on the Colonial Pipeline between the refineries and the Greensboro (label J) junction point. Note that in the 2016 pipeline disruption, only the cities F, G, H, I were identified as having a significant surcharge, whereas in the 2017 hurricane season, a significant surcharge is also identified in the cities of Jackson (label D) and Birmingham (label E). The result shows the distinction between the effects of a disruption at a precise point in the pipeline, which we examined in the previous subsection, versus the effects of the closure of the entire pipeline, which is what occurred in 2017. Like the 2016 pipeline disruption, however, we find that all locations downstream of the Greensboro junction experience relatively negligible amounts of surcharge, highlighting the importance of the Plantation Pipeline which remained fully operational during this period.

Second, we find that surcharges in Florida again reflect what is expected from the pipeline disruptions. In particular, the surcharge values do not rise at the same time and as sharply as the other cities, highlighting that the inland pipeline disruptions do not have a major impact on prices in Florida. However, unlike 2016, we do find positive congestion surcharges, reflecting the reduced port operations and limited marine movements of tankers due to Hurricane Harvey and Hurricane Irma. Nonetheless, the estimated surcharge values among the cities in Florida are much lower in magnitude than those of the more inland cities. This is likely a result of the flexibility of tankers and marine transport, where capacity can ramp up quickly and deliveries from other coastal ports can be accommodated (EIA 2017b).

Third, unlike the surcharge estimates in the previous section, the surcharges in 2017 appear more erratic, which may reflect the many simultaneously occurring disruptions in the network. A sustained surcharge estimate is observed in Nashville (label G) over this period, which is the only city served by pipelines but which does not lie in proximity to the Plantation Pipeline. The surcharge values in all other cities exhibit a generally decreasing trend after the onset of the disruptions, lasting for roughly two full months before dissipating.

Interestingly, the magnitude of surcharge estimates found during the 2017 disruptions appear lower in magnitude than those from the 2016 disruption, despite the far more disastrous consequences of the hurricane season. Examining the average price of gasoline across all cities offers an explanation. In 2016, the average price of gasoline during the month of the disruption (September 2016) was 2.09 USD/gallon whereas that of the month before (August 2016) was 2.01 USD/gallon. On the other hand, in 2017 the average price of gasoline was 2.55 USD/gallon during the first month of the disruption (September 2017), which is significantly higher than the average price of 2.20 USD/gallon in August 2017. This observation highlights the difference between the effects of market forces (i.e., supply and demand) and the effect of the transportation network. In particular, the major refinery (supply) disruptions resulted in the average price of gasoline increasing over *all* the cities while the disruption of the transportation network resulted in the estimated price disparities *between* the cities.

7. Discussion and Conclusion

This paper provides a theoretical and empirical study of the relationship between the logistical network of a market and spatial price integration. Key theoretical results include characterizing a neutral band within which locational prices can vary independently as defined by parameters of the transportation network and a novel price decomposition which identifies market price, transportation, idiosyncratic and congestion charges. We analyze how the congestion surcharges arising from network bottlenecks can propagate through the network and develop a discrete optimization methodology leveraging the price decomposition to detect capacity related disruptions from pricing data. Through a case study of the U.S. gasoline market, we show that the methodology is capable of extracting spatiotemporal patterns associated with structural inefficiencies in the underlying transportation network. These results highlight the effect of network topology, flexible transportation and inventory availability on consumer prices and market integration, all of which have important policy implications. Furthermore, these results can be used to guide infrastructure investments. For example, the cumulative estimated surcharge provides an approximate upper bound on the value that additional pipeline capacity would have had in the presence of these disruptions.

A few simplifications were made in this paper in the hopes of developing insights and methods that are relevant over general commodity markets and market structures. For example, perfect competition is assumed so that relationships between equilibrium prices and general capacitated networks can be easily characterized. The methodology and case study presented also assume access to only widely available spatial pricing data. A promising avenue for future research is thus to develop more granular models and to use additional (but likely privately owned) data to acquire more precise estimates of various market characteristics.

References

Balke, Nathan S, Thomas B Fomby. 1997. Threshold cointegration. *International economic review* 627–645.

Barrett, Christopher B, Jau Rong Li. 2002. Distinguishing between equilibrium and integration in spatial price analysis. *American Journal of Agricultural Economics* **84**(2) 292–307.

Bennett, Max, Yue Yuan. 2017. On the price spread of benchmark crude oils: A spatial price equilibrium model. Available at SSRN: https://ssrn.com/abstract=2894389.

Brown, Stephen PA, Mine K Yücel. 2008. What drives natural gas prices? *The Energy Journal* 45–60.

Cremer, Helmuth, Farid Gasmi, Jean-Jacques Laffont. 2003. Access to pipelines in competitive gas markets. *Journal of Regulatory Economics* **24**(1) 5–33.

De Vany, Arthur, W David Walls. 1993. Pipeline access and market integration in the natural gas industry: Evidence from cointegration tests. *The Energy Journal* 1–19.

Dieckhöner, Caroline, Stefan Lochner, Dietmar Lindenberger. 2013. European natural gas infrastructure: the impact of market developments on gas flows and physical market integration. *Applied energy* **102** 994–1003.

Dukhanina, Ekaterina, Olivier Massol. 2018. Spatial integration of natural gas markets: a literature review. *Current Sustainable/Renewable Energy Reports* 1–9.

EIA, U.S. Energy Information Administration. 2016a. Major gasoline pipeline in southeast disrupted for second time in two months. https://www.eia.gov/todayinenergy/detail.php?id=28632.

EIA, U.S. Energy Information Administration. 2016b. Pipeline disruption leads to record gasoline stock changes in southeast, gulf coast. https://www.eia.gov/todayinenergy/detail.php?id=28172.

EIA, U.S. Energy Information Administration. 2017a. Hurricane harvey caused u.s. gulf coast refinery runs to drop, gasoline prices to rise. https://www.eia.gov/todayinenergy/detail.php?id=32852.

EIA, U.S. Energy Information Administration. 2017b. Hurricanes harvey and irma lead to higher gasoline prices in florida. https://www.eia.gov/todayinenergy/detail.php?id=32932.

EIA, U.S. Energy Information Administration. 2019. Federal and state motor fuels taxes. https://www.eia.gov/petroleum/marketing/monthly/xls/fueltaxes.xls.

Ejrnaes, Mette, Karl Gunnar Persson. 2000. Market integration and transport costs in france 1825–1903: a threshold error correction approach to the law of one price. *Explorations in economic history* **37**(2) 149–173.

Fackler, Paul L, Hüseyin Tastan. 2008. Estimating the degree of market integration. *American Journal of Agricultural Economics* **90**(1) 69–85.

Gabriel, Steven A, Shree Vikas, David M Ribar. 2000. Measuring the influence of canadian carbon stabilization programs on natural gas exports to the united states via a 'bottom-up'intertemporal spatial price equilibrium model. *Energy Economics* **22**(5) 497–525.

Goletti, Francesco, Raisuddin Ahmed, Naser Farid. 1995. Structural determinants of market integration: The case of rice markets in bangladesh. *The Developing Economies* **33**(2) 196–198.

Goodwin, Barry K, Nicholas E Piggott. 2001. Spatial market integration in the presence of threshold effects. *American Journal of Agricultural Economics* **83**(2) 302–317.

Harker, Patrick T. 1986. Alternative models of spatial competition. *Operations Research* **34**(3) 410–425.

Harker, Patrick T, Terry L Friesz. 1985. The use of equilibrium network models in logistics management: with application to the us coal industry. *Transportation Research Part B: Methodological* **19**(5) 457–470.

Hendry, David F, Katarina Juselius. 2000. Explaining cointegration analysis: Part 1. *The Energy Journal* 1–42.

Hendry, David F, Katarina Juselius. 2001. Explaining cointegration analysis: Part ii. *The Energy Journal* 75–120.

Holmes, Mark J, Jesús Otero, Theodore Panagiotidis. 2013. On the dynamics of gasoline market integration in the united states: Evidence from a pair-wise approach. *Energy Economics* **36** 503–510.

ICF. 2016. East coast and gulf coast transportation fuels markets. Tech. rep., U.S. Energy Information Administration.

Lo, Ming Chien, Eric Zivot. 2001. Threshold cointegration and nonlinear adjustment to the law of one price. *Macroeconomic Dynamics* **5**(4) 533–576.

Lochner, Stefan. 2011. Identification of congestion and valuation of transport infrastructures in the european natural gas market. *Energy* **36**(5) 2483–2492.

Martínez-de Albéniz, Victor, Josep Maria Vendrell Simón. 2017. A capacitated commodity trading model with market power. *Real Options in Energy and Commodity Markets*. World Scientific, 31–60.

Massol, Olivier, Albert Banal-Estañol. 2016. Market power and spatial arbitrage between interconnected gas hubs .

McNew, Kevin, Paul L Fackler. 1997. Testing market equilibrium: is cointegration informative? *Journal of Agricultural and Resource Economics* 191–207.

Mudrageda, Murthy, Frederic H Murphy. 2008. Or practice—an economic equilibrium model of the market for marine transportation services in petroleum products. *Operations Research* **56**(2) 278–285.

Negassa, Asfaw, Robert J Myers. 2007. Estimating policy effects on spatial market efficiency: An extension to the parity bounds model. *American Journal of Agricultural Economics* **89**(2) 338–352.

Oliver, Matthew E, Charles F Mason, David Finnoff. 2014. Pipeline congestion and basis differentials. *Journal of Regulatory Economics* **46**(3) 261–291.

Park, Haesun, James W Mjelde, David A Bessler. 2007. Time-varying threshold cointegration and the law of one price. *Applied Economics* **39**(9) 1091–1105.

Parsley, David C, Shang-Jin Wei. 1996. Convergence to the law of one price without trade barriers or currency fluctuations. *The Quarterly Journal of Economics* **111**(4) 1211–1236.

Paul, Rodney J, Dragan Miljkovic, Viju Ipe. 2001. Market integration in us gasoline markets. *Applied Economics* **33**(10) 1335–1340.

Samuelson, Paul A. 1952. Spatial price equilibrium and linear programming. *The American economic review* **42**(3) 283–303.

Secomandi, Nicola. 2010. On the pricing of natural gas pipeline capacity. *Manufacturing & Service Operations Management* **12**(3) 393–408.

Takayama, Takashi, George G Judge. 1964. Equilibrium among spatially separated markets: A reformulation. *Econometrica: Journal of the Econometric Society* 510–524.

Appendix A: Proofs

Proof of Lemma 1 We first prove that $\lambda_s \leq \min\{\lambda_k + p^q_{ks} + \nu^q_{ks} \mid \forall k \in \mathcal{K}(s),\ q \in \mathcal{P}_{(k,s)}\},\ \forall s \in \mathcal{S}$. For any node s, there exists a path from every $k \in \mathcal{K}(s)$ to s, by the definition of $\mathcal{K}(s)$. Thus equations (4) and (5) must hold for each of these producer-consumer pairs $(k,s),\ \forall k \in \mathcal{K}(s)$, i.e., $\lambda_s \leq \lambda_k + p^q_{ks} + \nu^q_{ks},\ \forall k \in \mathcal{K}(s)\ ,\ \forall q \in \mathcal{P}_{(k,s)}$. This completes the first part of the proof. We now show that when $b_s > 0$ in the optimal allocation, $\lambda_s \geq \min\{\lambda_k + p^q_{ks} + \nu^q_{ks} \mid \forall k \in \mathcal{K}(s),\ q \in \mathcal{P}_{(k,s)}\}\ \forall s \in \mathcal{S}$. We invoke equilibrium condition (3). Since there is positive consumption at the consumer node s, there must exist at least one path of positive flow from some producer $k^* \in K(s)$ to s in an optimal market outcome; we denote one of these paths as q^*. By complementary slackness, $w_{ij} = 0$ for all (i,j) in path q^*. From equation (3), this implies that $\lambda_s - \lambda_{k^*} = p^{q^*}_{k^*s} + \nu^{q^*}_{k^*s}$. Rewriting this equation, we obtain $\lambda_s = \lambda_{k^*} + p^{q^*}_{k^*s} + \nu^{q^*}_{k^*s} \geq \min\{\lambda_k + p^q_{ks} + \nu^q_{ks} \mid q \in \mathcal{P}_{(k,s)},\ k \in \mathcal{K}(s)\}$. □

Proof of Lemma 2 Suppose that the set $\mathcal{S}_I$ represents the set of structurally integrated consumers. By Corollary 1, $\lambda_s = \min\{\lambda_k + p^*_{ks} | k \in \mathcal{K}(s)\},\ \forall s \in \mathcal{S}_I$. Since we are ignoring transportation costs, i.e., $p^*_{ks} = 0\ \forall k \in \mathcal{K}(s)\ \forall s \in \mathcal{S}_I$, then $\lambda_s = \min\{\lambda_k \mid k \in \mathcal{K}(s)\}$. Finally, since $\mathcal{K}(s)$ is the same for all $s \in \mathcal{S}_I$, the equilibrium prices λ_s must all be equal, i.e., $\lambda_s = \lambda'_s\ \ \forall s, s' \in \mathcal{S}_I$. □

Proof of Theorem 1 ($\Rightarrow$) We first show that price differences between s and r cannot exceed this bound for any set of feasible welfare and cost functions. Since s and r are structurally integrated, by definition both s and r have access to the same set of suppliers $k \in \mathcal{K}_{(s)}$. Since we assume that each consumer $s \in \mathcal{S}$ has positive consumption in the optimal market outcome, we let $\hat{k} \in \mathcal{K}_{(s)}$ denote a producer such that there exists flow from $\hat{k}$ to s in the optimal market outcome. From Equation (3), this implies that $\lambda_s = \lambda_{\hat{k}} + p^*_{\hat{k}s}$. From Corollary 1, this also implies that $\lambda_r \leq \lambda_{\hat{k}} + p^*_{\hat{k}r}$. The equations can be combined into the following inequality: $\lambda_s - \lambda_r \geq p^*_{\hat{k}s} - p^*_{\hat{k}r}$. However, since we do not specify $\hat{k} \in \mathcal{K}_{(s)}$, the following inequality must hold: $\lambda_s - \lambda_r \geq \min\{p^*_{ks} - p^*_{kr} | k \in \mathcal{K}(s)\}$. We can now make the same set of logical statements for the node r, thus bounding this inequality from the reverse direction. In doing so, we obtain the inequality $\lambda_s - \lambda_r \leq \max\{p^*_{ks} - p^*_{kr} | k \in \mathcal{K}_{(s)}\}$, which completes the proof.

($\Leftarrow$) We argue by contrapositive; suppose the network is not structurally integrated. We show now that for any non-structurally integrated network, it is possible to find feasible welfare and cost functions such that there does not exist a finite bound between price differences. Without loss of generality, suppose producer $\hat{k} \in \mathcal{K}(s)$ but $\hat{k} \notin \mathcal{K}_{(r)}$. Let the production cost functions be linear, of the form $W_k(b_k) = y_k b_k,\ \forall k \in \mathcal{K}_{(r)}$ and $W_k(b_{\hat{k}}) = y_{\hat{k}} b_{\hat{k}}$ for producer $\hat{k}$. When the set of cost function coefficients satisfy $y_{\hat{k}} + p^*_{\hat{k}s} \leq \min\{y_k + p^*_{kr} \mid \forall k \in \mathcal{K}_{(r)}\} + \epsilon$, the prices satisfy $\lambda_s \leq \lambda_r + \epsilon$ in the equilibrium. This is obtained by using Corollary 1, which states that $\lambda_s \leq y_{\hat{k}} + p^*_{\hat{k}s}$ and

$\lambda_k = \min\{y_k + p^*_{kr} \mid \forall k \in \mathcal{K}_{(r)}\}$. Thus, by considering cost functions that satisfy increasing values of ϵ, we can increasingly drive apart the values λ_s and λ_r; the price difference thus cannot be bounded. □

Proof of Proposition 1 Let Δ be some arbitrary value within the neutral band for a pair of structurally integrated consumers $s, r \in \mathcal{S}_I$, i.e.,

$$\min\{p^*_{ks} - p^*_{kr} \mid k \in \mathcal{K}_{(s)}\} \leq \Delta \leq \max\{p^*_{ks} - p^*_{kr} \mid k \in \mathcal{K}_{(s)}\}$$

Let $k_1 \in \arg\min\{p^*_{ks} - p^*_{kr} \mid k \in \mathcal{K}_{(s)}\}$ and $k_2 \in \arg\max\{p^*_{ks} - p^*_{kr} \mid k \in \mathcal{K}_{(s)}\}$ denote two producers shared by $s, r \in \mathcal{S}_I$. Let the production costs at all nodes $k \in \mathcal{K}$ be of the form $W_k(b_k) = y_k b_k$. Let

$$y_{k_2} = y_{k_1} + p_{k_1 s} - p_{k2r} - \Delta,$$

and let

$$y_k \geq \max\{p^*_{ks} + p^*_{kr} \mid k \in \mathcal{K}\} \ \forall k \in \mathcal{K} \backslash \{k^{min}, k^{max}\}.$$

Without loss of generality, we can normalize y_{k_1} by setting it to zero, i.e., $y_{k_1} = 0$. For all production cost functions that satisfy these conditions, all producer nodes except k_1 and k_2 become irrelevant; the production costs at other nodes are simply too high. Under these conditions, we claim that $\lambda_s = p_{k_1 s}$ and $\lambda_r = p_{k_1 s} - \Delta$, implying that $\lambda_s - \lambda_r = \Delta$. First, we need to show that for node s, buying and shipping from k_1 (with cost $p_{k_1 s}$) is less than buying and shipping from k_2 (with cost $y_{k_2} + p_{k_2 s}$). We prove this below:

$$\begin{aligned} y_{k_2} &= p^*_{k_1 s} - p^*_{k2r} - \Delta \\ &\geq p^*_{k_1 s} - p^*_{k_2 r} - p^*_{k_2 s} + p^*_{k_2 r} \quad \text{from def. of } k_2 \\ &= -p^*_{k_2 s} + p^*_{k_1 s}. \end{aligned}$$

This implies that $p^*_{k_1 s} \leq y_{k_2} + p^*_{k_2 s}$ and that in equilibrium, $\lambda_s = p^*_{k_1 s}$. Now, we show that for node r, buying and shipping from k_2 (with cost $y_{k_2} + p_{k_2 r}$) is less than buying and shipping from k_1 (with cost $p_{k_1 r}$). This is shown below:

$$\begin{aligned} y_{k_2} &= p^*_{k_1 s} - p^*_{k2r} - \Delta \\ &\leq p^*_{k_1 s} - p^*_{k_2 r} - p^*_{k_1 s} + p^*_{k_1 r} \quad \text{from def. of } k_1 \\ &= -p^*_{k_2 r} + p^*_{k_1 r}. \end{aligned}$$

Thus, in equilibrium, $\lambda_r = y_{k_2} + p^*_{k_2 r} = p^*_{k_1 s} - \Delta$. We have proved that for any Δ within the neutral band, there exists a set of cost functions for which $\lambda_s - \lambda_r = \Delta$.

Proof of Theorem 2 From equation (7), let

$$w_r - w_s = \max\{\lambda_r - \lambda_k - p^*_{kr} \mid k \in \mathcal{K}\} - \max\{\lambda_s - \lambda_k - p^*_{ks} \mid k \in \mathcal{K}\}.$$

Let $\hat{k} \in \arg\max\{\lambda_r - \lambda_k - p^*_{kr} \mid k \in \mathcal{K}\}$. Then

$$\begin{aligned} w_r - w_s &\le (\lambda_r - \lambda_{\hat{k}} - p^*_{\hat{k}r}) - (\lambda_s - \lambda_{\hat{k}} - p^*_{\hat{k}s}) \\ &= \lambda_r - \lambda_s + p^*_{\hat{k}s} - p^*_{\hat{k}r} \\ &\le \lambda_r - \lambda_s + \max\{p^*_{ks} - p^*_{kr} \mid k \in \mathcal{K}\}. \end{aligned}$$

Thus, $\lambda_s - \lambda_r \le w_s - w_r + \max\{p^*_{ks} - p^*_{kr} \mid k \in \mathcal{K}\}$. This completes the one side of the inequality. For the other inequality, let $\hat{k} \in \arg\min\{\lambda_k + p^*_{ks} \mid k \in \mathcal{K}\}$, and we use equation (8) to obtain

$$\begin{aligned} \lambda_s - \lambda_r &= \min\{\lambda_k + p^*_{ks} \mid k \in \mathcal{K}\} + w_s - \min\{\lambda_k + p^*_{kr} \mid k \in \mathcal{K}\} - w_r \\ &\ge \lambda_{\hat{k}} + p^*_{\hat{k}s} - \lambda_{\hat{k}} + p^*_{\hat{k}r} + w_s - w_r \\ &\ge \min\{p^*_{ks} - p^*_{kr} \mid k \in \mathcal{K}\} + w_s - w_r. \end{aligned}$$

This completes the proof. □

Proof of Proposition 2 Let $\hat{k} \in \mathcal{K}$ a producer for which the flow on (i,j) originates. Then

$$\begin{aligned} \lambda_j &= \lambda_{\hat{k}} + p^*_{\hat{k}i} + c_{ij} + \nu_{ij} \\ &\ge \min\{\lambda_k + p^*_{kj} \mid k \in \mathcal{K}\} + v_{ij}. \end{aligned}$$

From lemma 1 we see that

$$\begin{aligned} \lambda_j &= \min\{\lambda_k + p^q_{ks} + \nu^q_{ks} \mid k \in \mathcal{K}, q \in \mathcal{P}_{(k,s)}\} \\ &\le \min\{\lambda_k + p^q_{kj} \mid k \in \mathcal{K}, q \in \mathcal{P}_{(k,j)}\} + \nu_{ij} \\ &= \min\{\lambda_k + p^*_{kj} \mid k \in \mathcal{K}\} + \nu_{ij} \end{aligned}$$

Thus, $\lambda_j = \min\{\lambda_k + p^*_{kj} \mid k \in \mathcal{K}\} + \nu_{ij}$, and $w_j = \nu_{ij}$. □

Proof of Theorem 3 Recall that $\delta^{\min}_e(s) = \min\{\delta_e(k,s) \mid k \in \mathcal{K}\}$ and $\delta^{\max}_e(s) = \max\{\delta_e(k,s) \mid k \in \mathcal{K}\}$, where the value of $\delta_e(k,s)$ measures the cost difference between the minimum-cost path from k to s, and the minimum-cost path from k to s that does not include link e. When $\nu_e < \delta^{\min}_e(s)$, this by definition implies that any flow into s must have traveled on the link e, and hence incurred the full value of ν_e. Similarly, if $\nu_e = \delta^{\min}_e(s)$, then any flow into s must have either traveled on link e, or an alternative path that does not include link e but is at least as expensive as

$p^*_{ks} + \nu_e$, by the definition of $\delta_e(k,s)$. On the other hand, the definition of $\delta^{\max}_e(s)$ and equation (4) imply that for each $k \in \mathcal{K}$, there exists a path q which does not include link e from k to s such that $\lambda_s - \lambda_k \leq p^q_{ks} \leq p^*_{ks} + \delta^{\max}_e(s),\ \forall k \in \mathcal{K}$. Since path q does not include link e and therefore does not have any links with positive shadow price, this bound must hold, which implies that the congestion surcharge of node s with respect to link e must be less than or equal to $\delta^{\max}_e(s)$. □

Proof of Proposition 3 Let $r \in \mathcal{S}$ denote an arbitrary node for which to compare all other nodes with. Let $\eta^t = \lambda^t_r - w^t_r\ \forall t \in \mathcal{T}$, and let $\rho_s = \rho_{rs}$ and $\alpha_s = \alpha_{rs}$ denote the mid-point and half-width of the neutral band, as defined in Section 4.2. By equation (10), all prices in the market over any set of welfare and cost functions can be expressed in the form of equation (13). □

Appendix B: Supplemental Example for Section 4

We use a simple example to illustrate the difference between a pairwise and network neutral band in the setting where consumer nodes are directly connected. Suppose the market is represented by the network in Figure 9, where s_1, s_2 denote the two consumers in the market and k_1, k_2 denote the producers.

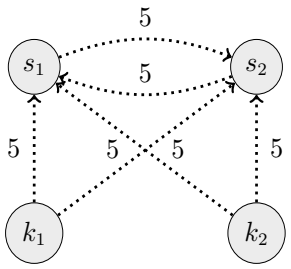

Figure 9 An example of a network where consumers are directly connected to each other.

Since there are direct links between s_1 and s_2 with transportation cost equal to 5, the pairwise neutral band width has value 5. However, when examining the network holistically, equation (6) implies that the prices at s_1 and s_2 must always be equal. The example highlights the importance of considering the entire network even when analyzing subsets of market participants.

Appendix C: Supplemental Table for Section 6

Table 1 Summary statistics of daily gasoline prices per gallon for 2016 and 2017

		2016					2017				
Label	City, State	Mean	Std	Min	Max	Range	Mean	Std	Min	Max	Range
A	Houston, TX	1.93	0.17	1.51	2.16	0.65	2.21	0.12	2.04	2.53	0.49
B	Baton Rouge, LA	1.87	0.18	1.47	2.11	0.64	2.13	0.09	1.98	2.33	0.35
C	New Orleans, LA	1.93	0.18	1.52	2.14	0.62	2.18	0.10	2.03	2.42	0.39
D	Jackson, MS	1.89	0.16	1.49	2.12	0.63	2.13	0.12	1.94	2.44	0.50
E	Birmingham, AL	1.91	0.19	1.49	2.17	0.68	2.14	0.14	1.94	2.5	0.56
F	Atlanta,GA	2.21	0.20	1.76	2.62	0.86	2.42	0.15	2.24	2.91	0.67
G	Nashville, TN	2.02	0.21	1.52	2.35	0.83	2.25	0.16	2.07	2.68	0.61
H	Columbia, SC	1.90	0.16	1.54	2.11	0.57	2.11	0.15	1.87	2.56	0.69
I	Charlotte, NC	2.04	0.16	1.67	2.26	0.59	2.28	0.14	2.06	2.65	0.59
J	Greensboro, NC	2.07	0.18	1.66	2.33	0.67	2.30	0.12	2.13	2.63	0.50
K	Raleigh, NC	2.09	0.15	1.73	2.31	0.58	2.30	0.13	2.10	2.62	0.52
L	Richmond, VA	1.94	0.19	1.48	2.17	0.69	2.19	0.11	2.00	2.50	0.50
M	Virginia Beach, VA	1.95	0.19	1.51	2.21	0.70	2.18	0.12	2.00	2.52	0.52
N	Jacksonville, FL	2.05	0.16	1.68	2.35	0.67	2.33	0.14	2.11	2.71	0.6
O	Orlando, FL	2.06	0.18	1.64	2.35	0.74	2.32	0.15	2.05	2.72	0.67
P	Tampa, FL	2.06	0.16	1.66	2.41	0.75	2.32	0.16	2.02	2.73	0.71
Q	Miami, FL	2.22	0.16	1.83	2.46	0.63	2.46	0.14	2.24	2.79	0.55